Journal of the Brazilian Society of Mechanical Sciences and Engineering (2021) 43:103
https://doi.org/10.1007/s40430-021-02854-4

REVIEW

Laser transformation hardening of various steel grades using different laser types

G. Muthukumaran[1] · **P. Dinesh Babu**[1]

Received: 20 July 2020 / Accepted: 22 January 2021 / Published online: 30 January 2021

Abstract
Laser surface hardening has become a promising replacement technique for conventional heat treatment. The laser is a heat source, deployed with optics to modify the surface along with the desired geometry. Laser density and its interaction time can be controlled and varied depending upon the final requirement at the surface. Increased hardness, diffusion-less phase transformation, self-quenching, uniform case depth over the entire scanned area are the reasons for laser-assisted hardening to become very popular and successful. Another reason for its success is that there is no bulk transformation of the material; only selected regions are subjected to laser irradiation for better surface improvements. This paper is a precis of various investigations done with a gas type CO_2 laser, a solid-state Nd: YAG laser, high-power diode laser and fiber laser (only Continuous Wave mode) over a variety of steel grades. Laser wavelength, power intensity, transverse/scanning speed, focal plane distance, surrounding atmosphere, pre-treated surface and surface absorptivity are parameters involved in laser surface hardening technique. By varying these independent variables, the desired surface property is achieved on the substrate subjected. A significant analysis of various experimental investigations done in this area is provided. Particular reference is made to surface hardening using different lasers as mentioned above. Although laser hardening is a potential technique for enhancing the surface properties, multi-track hardening/back tempering of the large surface area is still a concern and needs some attention. The main reason is a decrease in hardness in the overlap region. Various studies indicate that a single-track laser hardened region results in 3- or 4-times higher hardness than that of the original or base metal hardness. In contrast, in the overlapped region, the hardness value decreases, i.e., the difference between the hardness values at the single-track hardened region and an overlapped region is around 100–400 HV. This article reviews the chronological development of laser transformation hardening method explicitly by outlining the effect of process parameters on hardened depth and width, hardening influence in wear and corrosion resistance, numerical simulation and experimental validation techniques. Particular reference is made to CW (continuous wave) type laser hardening.

Keywords Surface hardening · Fiber laser · High-power diode laser · Nd: YAG laser · CO_2 laser · Case depth · Case width · Vickers's hardness · Residual stress · Back tempering

1 Introduction

Surface modification of metals with the laser has become a better alternative for manufacturing industries. Laser surface modification is a contactless process that delivers a clean manufacturing environment and results in superior-quality products with high volume and reasonable manufacturing cost. The laser beam is a beam of light, which is independent of the workpiece subjected, easily controlled, requires no particular environment like a vacuum and generates very intense energy fluxes at the substrate and also results in high temperature gradient between substrate and laser source. This temperature gradient is adequate to negate the need for

Technical Editor: Dr. Izabel Fernanda Machado.

✉ P. Dinesh Babu
dineshbabu@mech.sastra.edu

G. Muthukumaran
muthukumaran.g@mech.sastra.edu

[1] School of Mechanical Engineering, SASTRA Deemed University, Thanjavur 613401, India

an external quench medium. The first industrial application of laser was carried out at General Motors in 1973. CO_2 laser was employed to carry out surface hardening of gear housing [1]. Minimum distortion, uniform case depth over the entire substrate, self-quenching, speed and accuracy are some of the benefits of laser surface hardening process [2]. Most of the conventional hardening techniques are bulk transformation processes, i.e., the entire workpiece/sample has to be heat treated depending upon the application, and sometimes, it also involves secondary heat treatment to control the hardness at the surface. In comparison, the laser technique is a single-step process, i.e., it involves the interaction of laser source and surface only. This is the most desirable requirement for industries to enhance the mechanical properties and performance of a component [2].

Low power density and minimum interaction time are the two important characteristics of the laser hardening process. Majority of the incident infrared energy is reflected away if the power density is less than 10^5 W/cm^2. This situation can be overcome if the substrate is applied with black coating in order to increase the absorptivity of the metal subjected. One of the most influential parameters is absorptivity, which is directly affects the laser treatment method. Even though much work on absorptivity has been reported, it is not easy to identify a precise absorptivity because the surface depends on many parameters, such as substrate surface irregularities, laser beam irradiation angle and coating [3]. Absorption of the laser at the surface of the steel largely depends on the wavelength of irradiation; the absorptivity varies inversely with the wavelength [4]. Carbon dioxide gas laser, Neodymium-doped Yttrium Aluminum Garnet (Nd: YAG) solid-state laser, high-power diode laser and fiber laser are the four laser sources used in laser surface modification. The CO_2 laser is the one that offered the combination of power density and interaction time necessary for laser surface hardening of steels for industrial applications during the last century. Due to its high wavelength (10.6 µm), it offers a very low interaction time with the metallic surface, and due to this constraint, application of coating over the substrate has become mandatory for a few cases. Coating parameter, along with power density and interaction time, has become an integral part of CO_2 laser surface treatment technique. Predicting absorptivity after painting or coating is very difficult because it involves other parameters such as surface topography and laser irradiation angle. In the 1990s, Nd: YAG solid-state laser has become better substituent for gas type CO_2 laser. Shorter wavelength, low energy loss and flexible delivery of the laser beam are some of the advantages of Nd: YAG laser when compared with the CO_2 laser. The wavelength of Nd: YAG laser (1×06 µm) permits the beam to enter through an optical fiber with negligible energy loss on to the surface. Recent advancements such as multi-kilowatt diode lasers with 0·8 µm wavelength have become popular. Also, it can be attached to a robot to perform hardening of components with complex profile and geometry. Nd: YAG solid-state laser is the go-to laser for various steel and its alloys [5]. Special shaping optics were also developed to generate the required geometry of the laser beam with relatively uniform energy distribution on the surface [6].

In recent times, fiber lasers have been established and adapted for surface modification technique. In a typical fiber laser system, doping of active gain medium with rare-earth elements such as erbium, ytterbium, neodymium, dysprosium, praseodymium, thulium and holmium is done. Two technical developments, namely the use of single-mode fibers with significant transmissive function and high level of pumping, have amplified the power level to a large extent. These are the main reasons for selecting fiber laser as a source for surface hardening. When compared with Nd: YAG laser, fiber lasers have excellent stability and low cost of operation [7, 8].

Complex phenomena such as scanning speed, laser power density, focal plane position, interaction time, substrate absorption are difficult to understand from only experimental results. Therefore, several analytical models and numerical simulations have been applied to understand those complex phenomena. To date, several reviews have been done on laser hardening focused on experimental work. However, to the knowledge of the authors there is no published work that only focused on the review of CW type laser hardening of various steel grades, the chronological development of numerical models on laser transformation hardening technique. Therefore, this review focuses on the same. This review is divided into eight sections. In the first four sections, an overall idea about Laser hardening process is given using all the four types of CW mode laser system. In Sections five to eight, influence of LTH on wear and corrosion behavior of various steel grades, effect of laser parameters on the geometry of the hardened region, numerical simulation on LTH and industrial applications are discussed, and the final section discusses upcoming scopes and challenges in laser hardening.

2 Laser heat treatment

Various modern applications of laser are illustrated in Fig. 1. Monochromatic, coherent, highly directional and high-power density are the main attributes of laser beam. Surface modification with such power density is advantageous over various conventional techniques. Power density and interaction time are two crucial independent input variables in any laser processing techniques. The irradiated laser beam power density and its interaction time with the selected substrate surface determine the heating and cooling cycle frequency of the

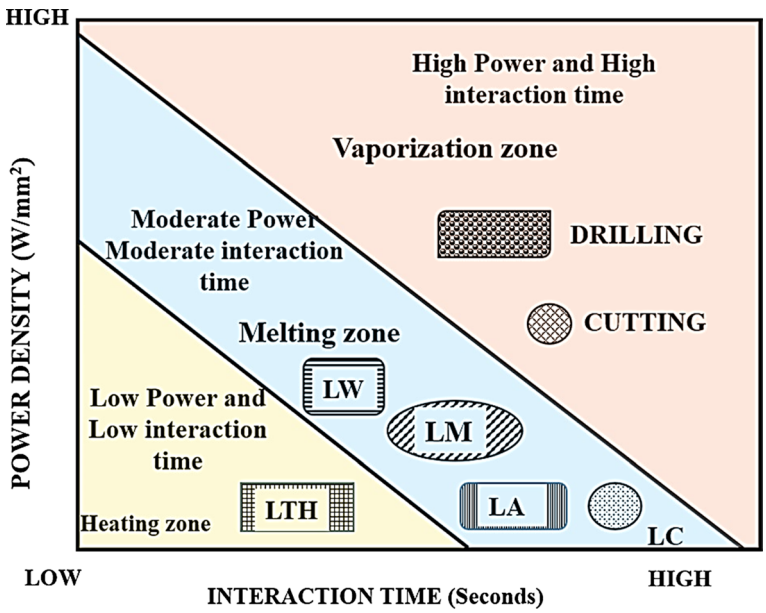

***LTH Laser Transformation Hardening; LW Laser Welding; LM Laser Melting; LA Laser Alloying; LC Laser Cladding**

Fig.1 Laser beam power intensity and dwell time of different laser material processing

process, which in turn determines the final microstructure of the laser-treated surface.

In Fig. 1, laser beam power density and interaction time of various laser material processing are listed. Based on the interaction between these two, laser material processing generally classified into hardening, melting and vaporization [9]. Figure 2 illustrates laser hardening process set-up and a cross-sectional view of the hardened region. These two layers can be easily distinguished from each other by their texture. Localized hardening of the substrate is made possible with the surface transformation hardening technique. The selected regions/localized area of the substrate/component is subjected to high-energy density laser interaction for a few seconds. This is achieved by making the laser head source traverse over the substrate at very high speed. During the time of interaction, laser beam hardens the surface by localized heating, and this step occurs swiftly and decreases the time for heat conduction of bulk material. The mechanism of transformation hardening involves austenitization and self-quenching, and this is considered to be one of the important characteristics and salient feature of laser material processing due to the diffusion-less transformation of martensite only on the selected regions/areas of the substrate/component without compromising toughness and ductility of the bulk. Homogenization of carbon in the austenite region is very crucial to steel quenching. Transformation hardening of steel is a time-dependent technique. In the event of laser surface hardening technique, substrate surface experiences high heating and cooling rates, which do not provide adequate time for proper homogenization of austenite. It is evident that the extended time is essential for the homogenization of austenite in high heating rates. The temperature of homogenization is fixed by identifying the melting temperature of the material primarily. As melting is not a desirable condition in laser transformation hardening (LTH), it is mandatory to know the relationship between heating rate, austenitization and homogenization temperature. In LTH, the homogenization temperature will always be higher than the austenitization temperature at higher heating rates [10]. Laser melting of the substrate/component also involves the same hardening mechanism of austenitization and self-quenching, with the only difference being an increase in interaction time of laser with the substrate surface which results in melting. Laser surface melting induces considerable case depth when compared with LTH. Case depth of the laser melted surface depends on power density, interaction time or scanning speed of the laser head. Case depth and case hardness can be easily controlled with the parameters mentioned above in laser material processing which in turn is very difficult in conventional heat treatment. Thermokinetic phase transformations in laser surface hardening involve only two steps, i.e., heating cycle (austenitization) and cooling cycle (self-quenching). In conventional heat

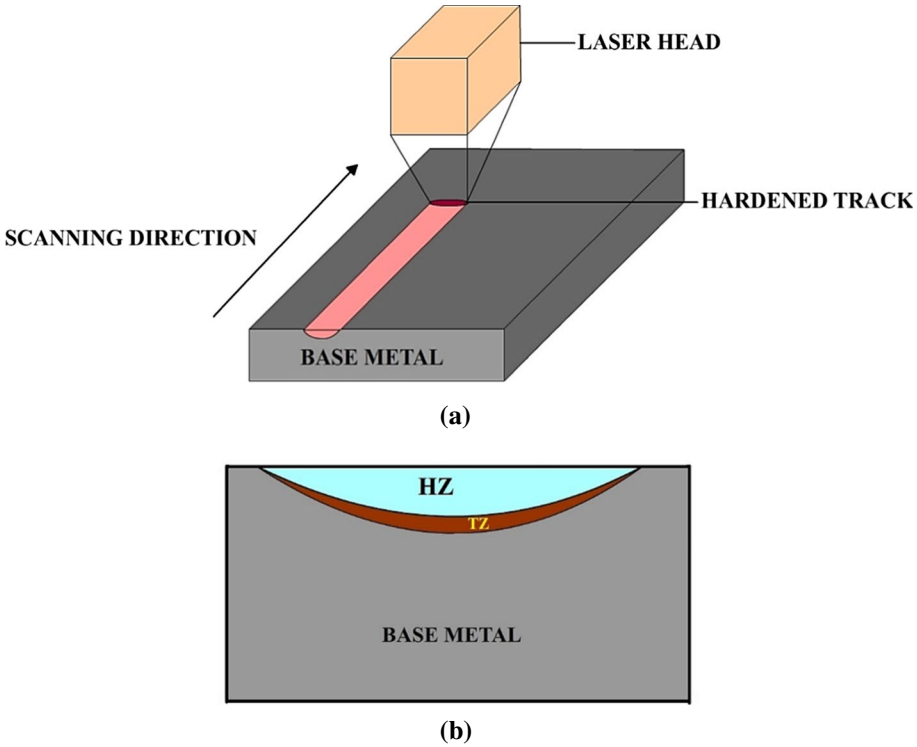

Fig. 2 **a** Laser hardening process set-up. **b** Laser hardening—a cross-sectional view

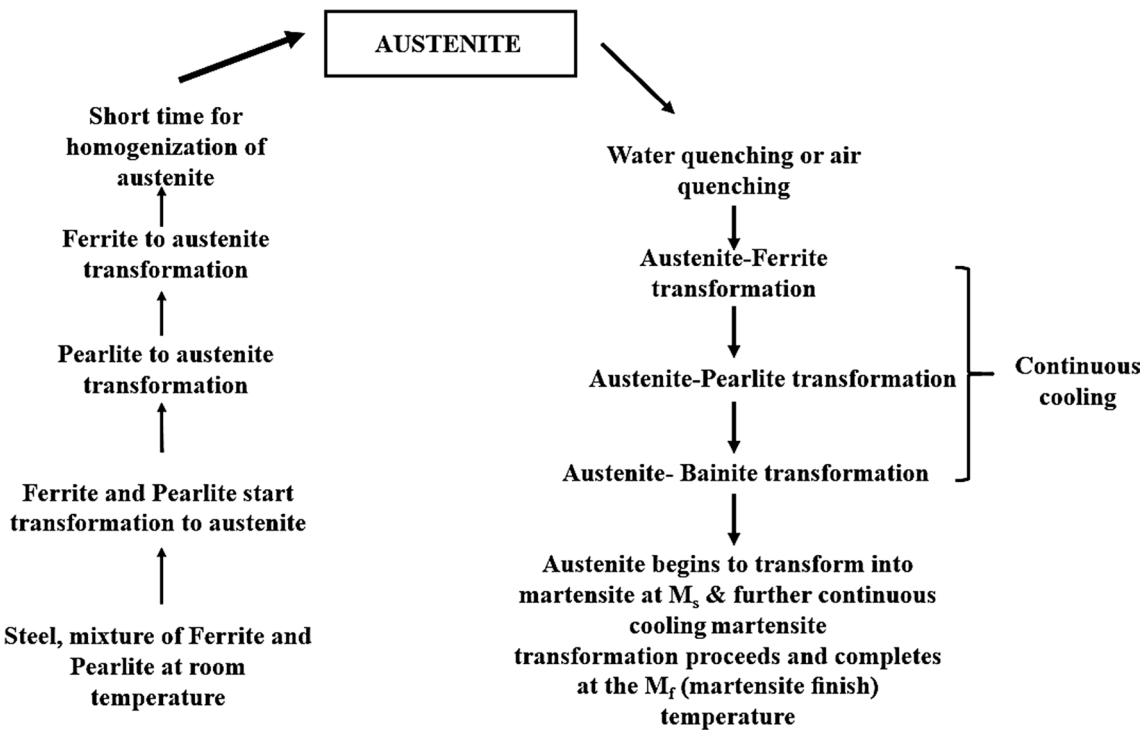

Fig. 3 Conventional hardening technique

treatment techniques, diffusion of carbon takes place at several stages. For instance, when steel is subjected to laser hardening and conventional hardening techniques for comparison, different thermokinetic phase changes are shown in Figs. 3 and 4.

In laser surface melting, maximum power density and high contact time between the laser source and the substrate surface are selected to achieve vaporization of the material. In laser shock peening, crack initiation and propagation are prevented by compressive residual stresses on to the substrate surface. The service life of some critical components which are used in aviation industries is extended by this technique. Recent advancement such as micro laser shock peening is extensively used to enhance the fatigue life period of micro-components used in MEMS, medical implants, micro-switches, relays, etc. One of the highlights of microlaser shock peening is that it does not require high-energy density laser systems to induce residual stresses on the surface. The uniqueness of the Laser hardening technique is that it achieves a constant case depth over the entire scanned surface and uniformity in residual stress distribution.

A 3D schematic diagram of a typical laser hardening process with two different beam geometries is shown in Fig. 5. In this process, a laser head moves with the laser beam at a certain scanning speed over a stationary substrate surface in *Z* direction.

3 Laser transformation hardening of various steel grades

The LTH process is carried out using four different laser types over various ferrous alloys, and some of these are extensively used for many critical/specific engineering applications. Fundamentals of the surface hardening technique, outlining some of its benefits compared with conventional hardening techniques and impact of shrouding gas atmosphere in laser hardening are discussed broadly in the following sections.

3.1 Surface treatment by CO_2 laser

Experimentation with gas type laser CO_2 for surface modification started in the early 1980s. Hardening of ferrous materials involves heat treatment and is still a challenging task. It involves in a primary process like raw material machining, suitable furnace treatment and several methods of cooling depending on the final applications of the material. All the hardening techniques certainly involves temperature concerns and consideration. The process like gas nitriding involves working in hazardous conditions, and it requires great attention and precision. Hardening technique like boronizing is a time-consuming process. Another way of surface modification carried on the ferrous materials is

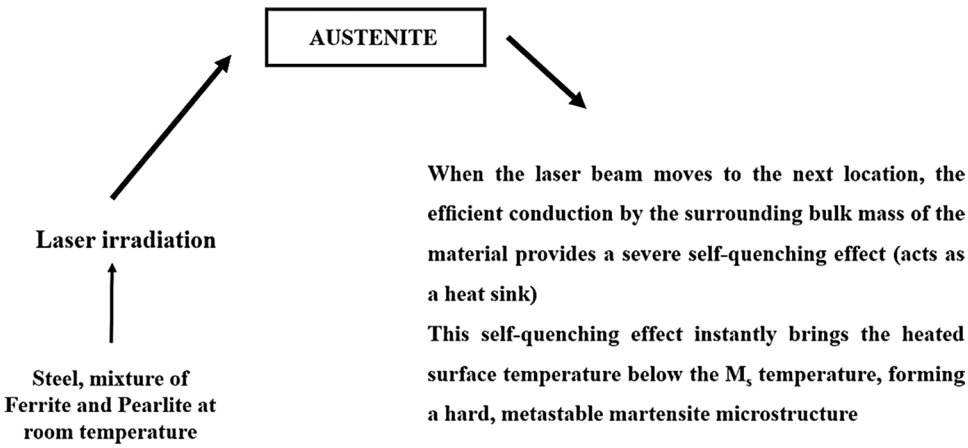

Fig. 4 Laser hardening technique

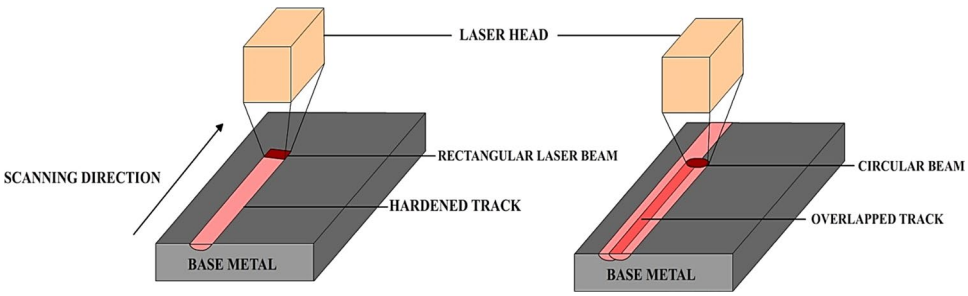

Fig. 5 **a** Single-track laser transformation hardening using a rectangular laser beam profile. **b** Multi-track laser transformation hardening using a circular laser beam profile

coating techniques, involving a separate set-up like vacuum and supply of inert gas atmosphere to carry out the trials. The resulting microstructure and properties from these techniques may or may not need fine alteration for its intended use. Laser technique overcomes all the hindrances in conventional hardening techniques and conventional surface treatment/modification techniques.

Laser surface hardening was carried out on AISI 1045 and AISI 4140 disk-shaped samples (diameter 40 mm and 4 mm thickness) using a 15-kW CW CO_2 laser. The samples were subjected to hardening and tempering before laser surface treatment. Line beams with 10×10 mm and 16×16 mm size and a circular beam of 8 mm diameter were carried out in this study. Tensile type residual stresses were induced/produced on the surface are due to a large temperature gradient between the laser source and material bulk. It is evident that in laser surface hardening track the residual stresses of thermal origin are always a tensile irrespective of the thickness of the sample considered [11].

X-ray diffraction characterization technique is used to find the residual stresses at the laser surface-melted 42CrMo4 steel. CW CO_2 laser irradiated on the pre-hardened 42CrMo4 steel. Case depth of 2.5 mm achieved in laser melting technique. Tensile stresses are induced at the laser melted surface/region, and compressive stresses occurred below the melted region [12].

Effect of a single longitudinal pass and two transverse passes at the center of the sample was carried out on the 50CrV4 steel. Before subjected to laser treatment, substrates/samples are hardened via oil quenching followed by tempering. Surface treatments were carried out using a 5 kW continuous CO_2 laser. The laser beam of square size 15×15 mm irradiated on the sample surface. Martensitic superficial layer with a hardness value of 700 $HV_{0.5}$ is achieved with laser hardening and a considerable increase in fatigue strength due to the internal longitudinal stresses created by uniform laser surface treatment. It also observed that the additional transverse pass carried out at the center causes a tempering effect and loss of fatigue resistance improvement [13].

Laser surface hardening of the piston ring groove of a ship's engine by CO_2 laser was analyzed in 1994. In this study, a CO_2 laser with a power 1000 W and line beam of dimension 5×5 mm irradiated on cast iron surface. Graphite coating was done on the cast-iron surface before laser hardening to increase the absorptivity. It has become evident that the hardened zone depends on the material and process parameters considered. Thermal stresses induced on the surface mainly due to the presence of large temperature gradient and martensite phase transformation. Tensile type residual stresses are observed at the hardened area, and compressive residual stresses are occurred/observed when the distance from the surface increased [14].

Laser surface hardening technique extended to EN31 steel in 1997. In this study, a 2-kW CW CO_2 laser with a beam diameter of 5 mm is used. Instead of surface coating, the EN31 steel was first treated for oil quenching at 840 °C and tempering at 150 °C before laser hardening. Uniform case depth of 0.4 mm is achieved over the entire laser-scanned area. The transition zone between the case hardened and the substrate is found to be 0.1 mm. Hardened surface/region consists of fine martensite structure with the hardness of 1000 HV. Instead of overlapping of laser tracks on the entire surface, hardened tracks with considerable spacing between them can provide an improvement in wear resistance [15]. Pre-hardened and black organic-coated 40CrNiMoA steel with tempered sorbite, a eutectic mixture of ferrite and cementite microstructure, subjected to laser quenching by a 2 kW CW CO_2 laser. Martensite and retained austenite are the microstructures obtained in the quenched zone. Coarser martensite structure obtained near the hardened/quenched surface. Width and depth of the laser quenched surface are 5.48 mm and 0.59 mm, respectively. The hardness of the quenched surface reached 750HV from 322HV [16].

Surface preparation by sandblasting and sandblasting with graphite coating was investigated using a low alloy 15CrNi6 steel. Surface preparation is mandatory in CO_2 laser hardening technique to achieve better absorptivity of the laser. Laser beam power, beam diameter, scanning speed and surface preparation are the chosen parameters for this study. A heat-affected zone (HAZ) consists of a very shallow layer and darkly etched region with the case depths of a minimum of 0.28 mm (without melting) and maximum up to 0.4 mm (with severe surface melting to a depth of 0.17 mm) obtained when the sandblasted sample irradiated. High power density and small beam diameter lead to increased HAZ depths. Laser carburizing was observed in sandblasting with graphite-coated sample with a minimum case depth of 0.59 mm (without melting) and 0.86 mm (with surface melting to a depth of 0.06 mm). Addition of graphite coating over sandblasted sample before laser treatment enhanced the surface absorptivity and resulted in greater HAZ depths. A very significant hardening effect was observed with the laser hardening technique. Lath martensite microstructure is in the sandblasted sample, and a carburized layer that consists of cementite, martensite plates and retained austenite microstructure in graphite-coated sandblasted sample was observed [17].

Laser hardening technique was carried out on structural CK60 steel using CO_2 laser having a power output of 3 kW and with beam diameters ranging between 4 and 6.5 mm. Rectangular sections of specimens with 4 mm thickness are exposed to 3.5% wt. NaCl solution at room temperature before laser treatment. The metallographic analysis revealed that the heat-affected zone had a case depth of minimum 0.05 mm to a maximum of 0.43 mm depending

on the laser conditions and martensite microstructure. It is evident that in laser hardening, during self-quenching austenite transforms to martensite. Near HAZ, a transition zone consisting of martensite, bainite and few traces of pearlite structure was observed. Overlapping, a reheating technique is also carried with ratios 0, 9, 21 and 38%. During overlapping, the hardened surface is once again reheated; as a result of reheating, it causes tempering of martensite and results in the final microstructure as tempered martensite. The hardness value of the as-received CK60 steel is 270 HV, and after laser hardening, the hardness value increased to 900 HV. Overlapping ratios with 0% and 38% exhibit better wear resistance results. Hardness value reported at the overlapped region is less than the single-track hardened region, and the value for the same is around 500 HV. In other words, 0% overlapping exhibits better wear behavior [18].

Sandblasted AISI 1045 steel is subjected for laser hardening using CW CO_2 laser. Power and scanning speeds are identified as processing parameters for this study. Laser hardening of the surface is carried out with a 0.16-kW power laser of beam diameter of 0.3 mm and scanning speeds of 0.26 m/s and 0.3 m/s. Reduction in heat-affected zone when the scanning speed is 0.3 m is evident that the interaction time between laser source and surface is minimized. Hardness values in the unaffected zone and heat-affected zones are 258HV and 768HV, which indicates that the hardened zone or hardened surface consists of a mixture of martensite and ferrite microstructure [19].

A thermo-absorptive coating was applied on the surface of the normalized En8 steel to enhance the laser absorption. 2.5 kW CW CO_2 gas laser with line beam dimension 15 mm x 1 mm irradiated on to the coated surface. Laser hardened specimens obtained a hardened layer of 0.14–0.25 mm case depth with a microhardness of 500–600 HV, which is comparatively higher than the initial value of 280 HV. Dry sliding wear test was carried out with the laser hardened specimen, and the results exhibited an enhanced wear resistance [20]. Case depth and width of the hardened layer depended upon power density and scanning speed of the laser beam [21].

C-30, C-40, C-45 carbon steels of dimensions 30×10x10 mm are subjected to laser surface hardening using 5-kW CW CO_2 laser. No coating of absorbent was applied on the substrate surface before, and after the laser treatment, instead, the entire laser hardening technique was carried out in a shielded environment using argon gas. In this experimental investigation, the identified independent input and dependent output variables are spot size of the laser beam, laser power, transverse speed and microhardness. Final microstructure and microhardness are highly influenced by the transverse speed of the laser beam and the percentage of the carbon content within the material [22].

A hypo eutectoid AISI 1045 coated with a thin layer of spray graphite is subjected for laser hardening. A CO_2 laser source with 8 mm beam diameter is used in this study. 50% overlapping with two passes, 70% and 75% overlapping with three passes are investigated in this study. The laser power of 1.1 kW with 8 mm beam diameter and 300 mm/min scanning speed is selected for 50% overlap, and laser power of 1.2 kW with 8 mm beam diameter and 400 mm/min scanning speed is selected for 70% and 75% overlap conditions. The third pass in the 75% overlap condition influenced the hardness. Overlapping leads to a softening effect of the hardened zone. To overcome this negative effect, a high-power source and a spot diameter of 8 mm are selected with a suitable scanning speed. It is evident that multiple passes with 75% slightly reduce the tempering effect in the hardened zone. The maximum hardness reported after 75% overlap with three passes on the top surface is 680HV, and almost the same value of hardness on the underside region of the irradiated surface and the case depth of the same is 0.5 mm [23].

The C45, 9Cr2Mo and W18Cr4V steel were investigated for softening phenomena in laser surface overlapping. All the three specimens were first sandblasted, then cleaned with acetone and coated with 10 wt.% hydroxyethylcellulose, 10 wt.% titanium dioxide powder and 80 wt.% talcum powder for better absorption. CW CO_2 laser with 4 kW power and 5.5 mm beam diameter is irradiated on all the three specimens with 20% overlap. Scanning speed of the laser beam is 4 m/min and a delay time of 5 min. was adopted between two passes. The delay was kept between the first pass and second pass of the laser beam to cool the samples down to the room temperature. Softening due to tempering is reported in the overlapping zone.

In C45 steel, microstructural analysis reveals that the hardened zone consists of typical lath martensite and a fraction of retained austenite, after the first pass. The overlapping zone comprises of tempered sorbite and tempered martensite microstructure. Needle-like martensite, retained austenite and fractions of carbide phase are found in W18Cr4V steel hardened zone. Tempered martensite, retained austenite and a small amount of carbide are the microstructures found in the overlapped zone. Residual austenite is reported at the laser hardened zone along with a large fraction of tempered martensite and carbide and comparatively less fraction of sorbite in 9Cr2Mo steel. The percentage of carbon in the base material influences the resulting microstructures. Martensite microstructure formed in the first pass transformed to tempered martensite during overlapping, and this may have happened because the highest temperature of the second pass is lower than the austenitized temperature of the steel. The average hardness of 45, 9Cr2Mo and W18Cr4V steel in the hardening zone is 760 HV, 955 HV and 908 HV comparatively very higher than the overlapped zone [24]. Hardness

values for the three materials, C45 steel, 9Cr2Mo steel and W18Cr4V steel at the overlapped regions are 400 ± 50 HV, 600 ± 50 HV and 750 ± 20 HV.

3.1.1 Precis

Surface absorption is a primary concern in CO_2 laser surface hardening since its wavelength is 10.6 µm. Surface preparation is mandatory in CO_2 laser hardening. Laser hardening involves high-temperature heating at the surface, and self-cooling, residual stresses are inevitable. Tensile stress is reported at the hardened zone, and compressive stress at the sections is below the hardened zone in laser hardening, and this is valid for almost all the ferrous materials.

3.2 Surface treatment by Nd: YAG laser

Conventionally heat-treated high nitrogen tool steel (HNS) X30CrMoN15 is subjected to laser hardening. HNS is exclusively used in bearings and gears in aeronautics. Tempering above 600 °C is done on HNS to gain toughness, and this leads to an adverse effect in the properties of the steel. A 3 kW Nd: YAG laser source was used in this study. Laser surface hardening was carried out under a special atmosphere of 15 l/min N_2 and 0.13 l/min O_2. Two passes were made on the base substrate. As a result of hardening, martensite microstructure is reported with significant improvement in wear resistant, and this may be due to increase in hardness at the laser hardened surface; tempering effect increases the wear rates at the overlapping zone. Compressive residual stress was reported within the hardened layer and tensile residual stress at the hardened surface [25].

Comparative study of 55Si7 and 50CrV4 steels is carried out. The process sequence is illustrated in Fig. 6.

Significant increase in the hardness around 800HV for 55Si7 and 730 HV for 50CrV4 is reported for both the materials after laser hardening. Increase in hardness has improved wear resistance for both the materials. 55Si7 showed better wear resistance than 50CrV4 [26].

Medium carbon steel SM45C subjected to laser surface hardening. A 4 kW Nd: YAG laser with optimized power irradiated on the surface. Laser beam focussed on the rod-shaped specimen which is held at the lathe chuck and rotated at an optimum speed. Laser beam head transverses over the rotating specimen and during the beam—surface interaction, a shielding gas was sprayed. The identified parameters for this process are power, beam diameter, rotating speed and beam transverse speed. Surface melting occurs at high power and low rotating speed. Overlap rate increases with the increase in the rotational speed and decreases in laser beam transverse speed. Case depth, width and overlap length increase with an increase in hardening tracks. Maximum case depth reported is 0.8 mm, and the hardness value is around 800HV at the hardened surface [27].

A disk opener made of 45 steel is subjected for laser hardening by HLD1001.5 solid-state lasers. Laser power, scanning speed and beam diameter are identified as working parameter in this study. By keeping scanning speed (0.3 m/min) and beam diameter (3 mm) as constant, laser power is varied and the identified laser power for the experiment are 400 W, 500 W and 600 W. The hardened layer consists of a melted zone, a phase transformation and a heat-affected zone. The maximum depth of the melted zone reported from all the three trials is 0.126 mm. Case depth is directly proportional to the laser power; with an increase in laser power case, depth increases. Maximum case depth of 1.044 mm is observed when the laser power is 600 W, and a minimum depth of 0.736 mm is observed when the laser power is 400 W. Characterization analysis reveals martensite and fractions of retained austenite microstructure in the melted zone. Lath martensite and acicular martensite are in the phase transformation zone. 90% of the hardened layer was observed in the phase transformation zone. Ferrite and martensite are microstructures in heat-affected zones. HAZ microstructure is similar under all laser treatments. 770HV and & 700 HV are the reported hardness values after laser hardening with power 400 W, 500 W and 600 W. Maximum hardness is achieved with minimum laser power [28].

AF63CrMnMo6 forged steel is subjected to laser hardening. An Nd: YAG Rofin DY 044 laser with a variable output power of up to 4.4 kW and beam diameter 0.4 mm used in this study. Since 0.4 mm beam diameter is very low for

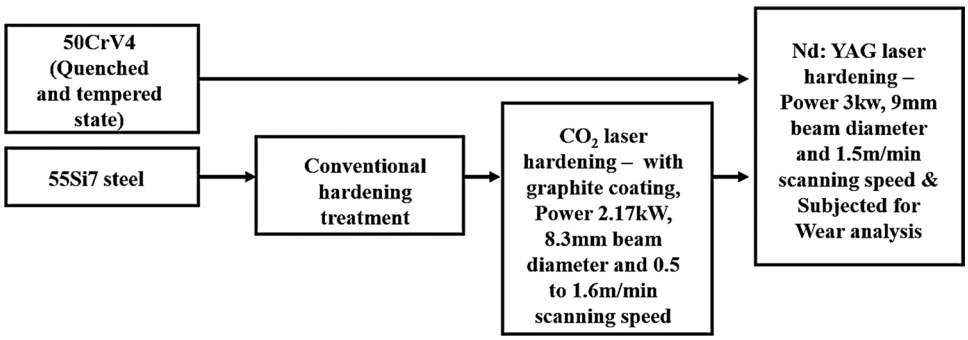

Fig. 6 Process sequence

industrial application, the beam diameter of the laser source increased to 15 mm by defocusing the lens. 0.3 m/min is the selected transverse speed of the laser beam over the surface. The base material, which is a hardened and tempered steel, consists of tempered martensite and secondary carbides microstructure. After laser hardening, the microstructure of the hardened layer consists of martensite and a fraction of retained austenite. Cross-section microstructure analysis reveals a hardened zone, transition zone, heat-affected zone. Maximum case depth of 2.4 mm is achieved by varying the identified process parameters. A maximum hardness value of 800HV is achieved [29].

Laser surface melting effects were studied on maraging steel since their mechanical properties make them an alternative to hot-working tool steels such as AISI H11 and H13. The maximum operating power of the laser is 4.4 kW with an optical fiber of 0.6 mm beam diameter. The identified operating parameters for surface melting are power 1–3 kW, scanning speeds 1.5 m/min, 3 m/min, 3.6 m/min and beam diameter 3–6 mm. In surface melting, interaction time between the laser and surface is considerably high when compared with transformation hardening. The above-identified scanning speeds range evident the same. Figure 7 illustrates various steps and conditions involved in the process.

2 kW power, 50 mm/s laser beam scanning speed and a 3 mm laser beam diameter are the selected process parameters, laser surface melting done on the surface without any cracks. Hardened/solidified zone, heat-affected zone and base metal are identified in the microstructural analysis at the cross-sectioned surface after laser melting. Microstructure depends on the constituents of the base metals, and in this case, titanium-rich particles are identified in the melted zone. Melted zone reported with very fine martensitic structures of cellular and dendritic solidification. The HAZ consists entirely of laser melted zone. 25% overlapping treatment also resulted in the same microstructures. Aging treatment after laser surface melting shows that martensite phase does not revert to the austenite phase. Microhardness reported after LSM treatment with hardened, and tempered steel is 365HV. There is no significant improvement in hardness of the material, and this may be due to the percentage of carbon in the base material. Significant decrease in microhardness is observed in pre-aged treatment steel after surface melting. Post-aging treatment slightly increases the hardness of the steel [30].

EN25 steel is considered for laser transformation hardening technique. CW Nd: YAG laser with 2 kW power as a source was used in this research. Power and scanning speed are the identified important parameters in this study. Melting is not a desirable condition in transformation hardening; to avoid such undesirability condition initial trials were conducted on the surface to finalize the optimum/working parameters. From the initial trials, it is concluded that at 75% laser power capacity irrespective of the scanning speed and 37.5% laser power capacity with a very low scanning speed (< 0.5 m/min) also melting occurs. Beam diameter of 1.55 mm is kept constant for the entire experimentation. Working parameters are identified and carried out using 32 FFD matrix methodology to run the experiment with the optimal parameters case depth of

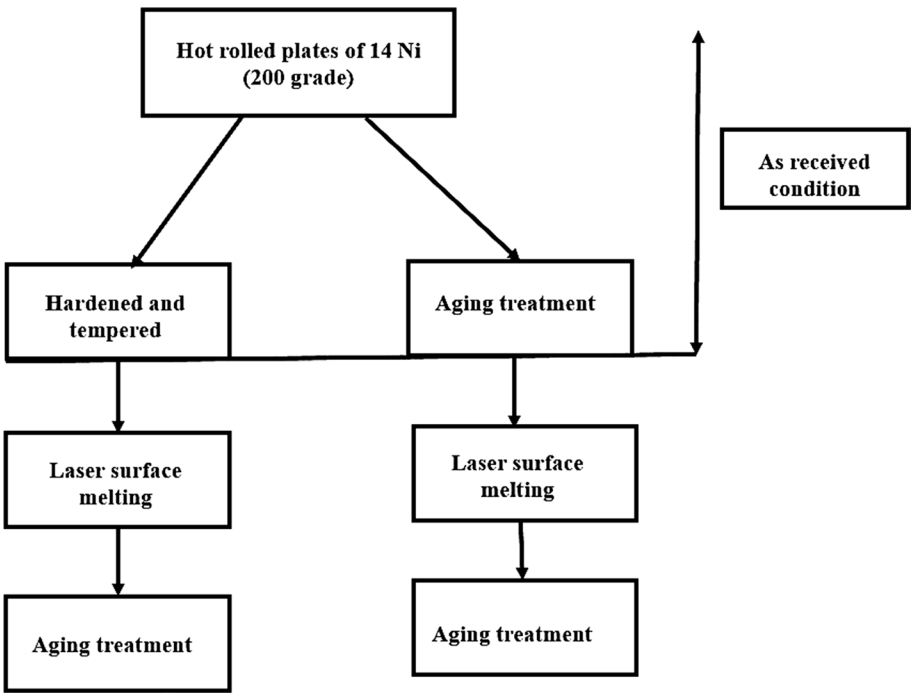

Fig. 7 Sequence and conditions involved in the process

0.65 mm achieved in laser hardening. Surface hardness after transformation hardening is in the range 760–780 HV [31, 32].

A high-chromium, high-carbon tool steel AISI D2 is subjected to laser hardening. Solid-state CW 2 kW Nd: YAG laser was used. Power, scanning speed and beam diameter are the identified process parameters in this study. Maximum case depth of 0.5 mm with 303HV hardness achieved at minimum power, minimum scanning speed and minimum 2 mm diameter and the maximum hardness of 490 HV with 0.35 mm case depth achieved at minimum power, minimum scanning speed and 3 mm beam diameter [33].

Quenched and tempered AISI 4140 steel is selected for laser surface hardening. Distance between the parallel tracks and effects of overlapping are the primary considerations in this study. Parameters power, scanning speed and beam diameter are kept constant. 4-mm and 5-mm overlap trials are carried out on the surface. Hardness value at the hardened surface is 800 and 500 HV at the overlapped surface. 1 mm (maximum) case depth is achieved with the identified parameters values. Regular phase transformation kinetics of laser surface hardening is reported in this study [34]. A continuous-wave 2 kW Nd: YAG laser irradiated on Cr12 mold steel. Laser hardening is carried out in the presence of Argon gas. The gas flow rate is kept constant for all the experiment trials. Case depth is influenced by laser power, scanning speed and focus/defocus distance. By varying the identified process variables, case depth of 1 mm is achieved. Laser power is operated at 30%, 50%, 75% and 100% capacities. Bead profile and case depth analysis are the interested candidates in this study [35].

3.3 Precis

Solid type Nd: YAG (Neodymium-doped: Yttrium Aluminum Garnet) laser with 1064 nm wavelength is a better replacement for CO_2 gas type laser for surface hardening. Surface absorptivity is comparatively high for Nd: YAG laser. Surface coating prior to surface treatment is not mandatory in Nd: YAG surface hardening. Case depth and width are comparable with CO_2 laser treatment. Loss of power is minimum in Nd: YAG laser, and its efficiency is comparatively higher than the CO_2 laser. Surface hardening treatment is carried out with an inert gas atmosphere resulted in considerable improvement in surface hardness and wear. Overlapping treatment on the substrate does not yield any improvement but a decrease in hardness in the overlapped zone.

3.4 Surface treatment by high-power diode laser (HPDL)

The wavelength, cost, efficiency, compact size, beam profile stability are some of the inherent qualities of the diode laser, which make them suitable for surface hardening of ferrous materials. Both CO_2 laser and Nd: YAG laser generate just a single beam, which results in fluctuations and irregular spikes in beam profiles, and this is not the case in diode laser since it has a high number of superimposed beams.

En8 and En24T steels are selected for laser surface hardening since both the materials have the same amount of carbon content in them. Laser hardening is done with a 1.2-kW diode laser. Power and scanning speed of the laser beam are the selected parameters for this work. A rectangular laser beam of 5 mm × 0.38 mm dimension is selected for this study. Working range of laser power is 400–100 W, and scanning speed is 0.1–1.6 m/min. Case depth of 0.2 mm is achieved in En8 steel and 0.5 mm in En31 steel, and this difference is may be due to the alloying elements in the base materials. A hardness value of 500 HV is achieved in En8 steel, which is comparatively lower than the En31 steel, whose hardness value is 800HV [36].

Wavelength is one of the important characteristics of the laser. Surface absorptivity is one of the main considerations in laser surface hardening. A typical CO_2 gas laser has a wavelength of 10.6 µm, and this is one of the reasons why we have to consider surface coating for better absorption prior to laser hardening. Compared with CO_2 laser, a solid-state Nd: YAG laser has the wavelength of 1.06 µm, and this is the reason why the absorptivity is considerably high in Nd: YAG laser when compared with a CO_2 laser. High-power diode laser (HPDL) is distinct from the above two different types of laser. Its wavelength is 0.8 µm. Laser surface hardening achieved with HPDL is free from surface melting, cracks and undesirable case depths [37].

Laser surface hardening feasibility is carried on the AISI 1536 steel. A 2.5 mm uniform case depth is achieved on a typically flat surface, while a 1.5 mm case depth is achieved on parts which have a groove of 2.0 mm radius. Significant improvement in the hardness in the order of > 650 HV is reported [38].

42CrMo4 low alloy steel and AISI 420L corrosion-resistant steels are subjected for laser hardening. Hardened and tempered are the as-received condition of the steels. Laser surface hardening is carried out by two different approaches. First, laser hardening of 42CrMo4 and AISI 420L steel is carried out in the presence of inert gas atmosphere Argon and secondly at normal atmospheric air. 40% absorptivity of 42CrMo4 and 38% absorptivity of AISI 420L are reported when hardening is carried out at inert gas atmosphere. Absorptivity of 42CrMo4 increases, when the laser hardening is done at normal atmospheric condition, i.e., in the presence of air. This may be due to, at higher interaction time between beam and surface, temperature increase and thus results in a thick oxide layer growth due to presence of oxygen, which in turn increases the surface absorptivity. There is no significant improvement in absorptivity in AISI

420L, and this may be due to the presence of chromium in the metal itself. Phase transformation depth/case depth of 42CrMo4 steel is comparatively higher than AISI 420L steel [39].

Laser hardening of X30CrMoN15 steel in a controlled atmosphere is the key consideration in this study. Laser hardening with a single track on the substrate surface in the presence of air resulted in 0.5 mm case depth, and the hardness for the same is 780 HV. When the substrate irradiated with laser in the presence of Argon gas, case depth of 1.2 mm with hardness around 650 HV is reported. Both the trials are carried with the same sets of operating parameters. Overlapping of 10% and 50% carried on the surface in the presence of Argon resulted < 650 HV hardness, and this may be due to tempering effect in the hardened zone, and there is no significant decrease in the hardened zone reported. In the case of overlapping in the atmospheric condition, at higher depth hardness value decreases due to tempering. For instance, a significant decrease in the hardness is reported after 0.15 mm depth [40].

Laser transformation hardening on AISI 1045 steel resulted in 0.4–0.45 mm case depth with the maximum hardness value around 600HV. Power density is directly proportional to the hardened depth. The resulted case depth is achieved with the power range 0.4–0.6 kW. By using ANSYS, the experiment is validated [41].

Conventional boronizing of steels involves heating a well-cleaned material for more than 10 h around 700–1000 °C. Boronizing is carried out on the surface to increase the surface hardness of a material for a certain depth by inducing FeB and Fe_2B layers. High hardness at the surface of the material makes it to be more brittle. In this study, S45C steel is selected for laser boronizing. Boron trioxide (B_2O_3) and Fe-B powders are mixed and coated over the surface in the order of 0.3–0.6 mm layer thickness and the same is dried with the help of infra-red heater. After laser treatment, the substrate is cleaned with acetone. Microstructural analysis reveals a good adhering of coating with the surface after laser irradiation. By altering laser power, boron concentration is altered, and the uniform distribution of boron is achieved in this process. Boron proportion in the hardened layer influences the surface hardness. Maximum case depth of 0.4 mm with 1220 HV hardness is achieved [42].

When laser hardening has to be done on a significantly large surface area, multi-track hardening is required. This process is known as overlapping or back tempering. A mathematical model to predict the overlapping in multi-track surface hardening and to calculate the hardness profiles is the fundamental objective of this study, and the same is validated by performing multi-track laser surface hardening on AISI 4140 steel with optimum parameters. After conducting preliminary trials, the identified parameter values are power 0.85 kW (69% absorptivity), scanning speed 0.5 mm/s, beam size 12 mm × 8 mm. 12 mm axis of the beam is made perpendicular to the direction of travel. Overlap tracks varied from 3 to 6 mm. After a simulation run, 5 mm overlap gave the best result with a minimum drop in hardness in the tempered zone/overlapped zone. With the identified parameters and overlap ratio, i.e., 58% (5 mm), laser hardening is processed at the surface. Predicted case depth is 1.9 mm in the simulated model, and the actual case depth obtained is 2 mm (without melting). Hardness value achieved at the surface is in the range of 668–700 HV, and in the tempered zone, the range is 480–570 HV [43].

Surface irregularities are inevitable in the conventional machining process. Suppose if the material is subjected to repetitive cycle load with some surface asperities, crack propagation and failure may happen during the operation, which leads to failure. A laser beam melts the peaks of asperities and fills the valley gaps of the surface, thereby reducing surface roughness, and this process is known as laser polishing. Laser polishing of AISI 1045 steel is carried out in an inert gas atmosphere Nitrogen. Case depth of 0.125 mm with 550HV hardness value is achieved in this microlayer melting process. Compressive residual stress is reported at the HAZ. Fatigue results revealed that laser polishing is an effective technique for the surface, having roughness value more than 35 µm only[44] (Table 1).

Comparative study of laser surface hardening and laser melting is carried on a hardened and tempered AISI H13 tool steel with 0.9 µm surface roughness. Laser processing is carried out in an inert gas atmosphere. A study reported that the laser density is directly proportional to the laser power and inversely proportional to scanning speed and focal distance. Power range is between 0.9 and 2.5 kW, scanning speed from 0.12 to 0.48 m/min and 285 mm distance of laser head from the surface selected for laser processing. A rectangular beam of size 20 mm × 5 mm is resulted after the focal distance setting. Four scenarios are reported by considering laser power density (i) if the laser power density > 75 J/mm^2, i.e., at 100 J/mm^2 melting occurs, (ii) if the laser power density is 75 J/mm^2, hardening occurs, (iii) if the laser power density is in the range 50–75 J/mm^2, hardening occurs and (iv) if the laser power density < 50 J/mm^2, laser irradiation on the surface is ineffective. Laser processing results in the melted zone, hardened zone and transition zone/HAZ. Microstructure analysis reveals that the melted region consists of dendrites, carbides, martensite and retained austenite. The hardened layer consists of martensite and carbide precipitates and coarse carbides in the heat-affected zone. Case depth of around 1.1 mm is achieved in laser hardening and more than 1.7 mm in laser melting. The average hardness value of laser hardened surface is 680 HV, and laser melted surface is 790 HV. Microtensile studies revealed that laser hardening technique is the best approach to achieve high yield strength of the material. Laser engineered surface

resulted in superior wear resistance and marginal corrosion resistance [45, 46] (Table 2).

CMn440 (%C < 0.1) automotive steel sheet subjected to laser surface hardening. Single-track and multi-track hardening was done on the substrate. Single-track hardening is conducted with constant power (0.7 kW) and varying scanning speeds (1.44 and 1.68 m/min). Case depth of 0.5 mm resulted with 1.44 m/min speed and 0.3 mm with 1.68 m/min, and this is due to the interaction time of the laser with the substrate. A significant improvement in the hardness is reported. Laser hardened surface hardness is around 370HV, comparatively higher than the base hardness value 150 HV [47] (Table 3).

A powerful diode laser is irradiated on the AISI 1040 steel surface to improve the fatigue life of segments. Cylindrical specimens held on to the chuck and rotated at optimum speed, and simultaneously, laser beam scanned over the surface with a speed range varies from 12 to 20 mm/s. Elliptical beam spot of major axis 1.9 mm and 0.6 mm minor axis is selected for this stud, to ensure the penetration of the laser beam on the surface focal distance of 63 mm identified. No significant impact of laser irradiation on the surface is reported at low power 0.1 kW and 0.15 kW. Melting trace on the surface is observed at low scanning speeds 12 and 14 mm/s at 0.2 kW power. At 0.2 kW power and scanning speeds 16, 18 and 20 mm/s hardening phenomena exist. Case depth of 0.15 mm with hardness value around 300 HV at hardened surface is reported after the hardening process. The hardened layer consists of annealed martensite. Fatigue analysis reveals that AISI 1040 is a potential contender for laser hardening to improve fatigue life [48].

By varying, energy power density of laser beam from 265 W/cm^2(min) to 1705 W/cm^2(max), laser tempering effect on 42CrMo4 is investigated. The cylindrical type specimen of size 200 mm length and 56 mm diameter is considered. Laser power and rotating speed are the parameters selected to carry out laser hardening. A rectangular laser beam of size 25.8 × 7.8 mm is made to irradiate on the surface. In this study, the laser beam is focussed on the substrate at a static position. The entire experiment is brought in to three laser power groups: Group 1 (265 W/cm^2, 425 W/cm^2, 585 W/cm^2), Group 2 (745 W/cm^2, 905 W/cm^2, 1065 W/cm^2) Group 3 (1225 W/cm^2, 1385 W/cm^2, 1545 W/cm^2, 1705 W/cm^2). Group 1 reported the hardness value range 580–650 HV. Group 2 reported the hardness value range 400–500HV. Group 3 reported the hardness value range 600–700 HV. Maximum hardness values reported in Group 1, Group 2 and Group 3 are 650 HV, 500 HV and 700 HV. Case depth of 0.9 mm is achieved at all the three power groups [49].

The abrasive wear resistance of 40Cr steel is enhanced by laser quenching with Argon atmosphere. A rectangular laser beam of size 25 mm × 6 mm is made to expose on the substrate surface. 1.15 kW laser power and 0.48 m/min transverse speed are the parameters selected for this process. The hardened layer has a case depth of 0.9 mm, and it comprises of high-temperature zone (high-temperature gradient exists at this zone which leads to the development of martensite and fractions of retained austenite) and medium temperature zone (traces of sorbite phases, bainite mixture and chromium carbides). The hardness value of 700 HV identified at the quenched layer [50].

Case depth achieved on the material after the laser type hardening process depends on irradiated laser beam power, scanning speed and distance of the focal plane. Location of the focal plane is another complex parameter that has to be considered. Laser beam interaction time with the surface depends on the length of the beam and its transverse speed over the substrate surface. Multi-response optimization technique resulted in optimum parameters to carry out laser hardening of AISI 4130 steel. Case depth of 1.3 mm with 800HV hardness value is achieved by experimenting with the optimized parameters. 30% and 50% overlapping is done on the surface. Experiments showed that 50% overlapping is comparatively significant than the other [51].

Laser hardening of AISI 410 and AISI 420 is carried out with identical parameters to compare the material behavior. Identical chemical composition of two selected materials is the crucial reason to do a comparative analysis. Scanning speed, focal plane position and power are the independent parameters while depth, hardness and width are the dependent parameters of this experimentation. Percentage of carbon influence the hardenability in both the materials selected. The hardness value of AISI 420 is 720 HV which is higher than AISI 410 hardness value 6500HV. Case depth of AISI 410 is higher than the AISI 420 steel, and this may occur due to alloying elements, surface absorptivity and thermal conductivity of the material itself [52].

Fretting tests were conducted on AISI P-20 improved steel to explore the effect of laser surface hardening done with a 4-kW power diode laser. A rectangular beam of dimension 24 mm × 1 mm is focussed on the surface with an average beam power of 1.25 kW and its corresponding laser density of 250 J/mm^2. The hardness value of the hardened surface is 700 HV at 0.5 mm depth, considerably higher than its base hardness value 300 HV. Maximum case depth of 0.7 mm attained with laser hardening. Laser hardened sample showed reduced values for the coefficient of friction and wear volume than the base metal. Moreover, laser-processed samples have smoother surfaces with tiny abrasion grooves on the surface [53].

Laser quenching of 1.0C–1.5Cr steel is carried out on four different specimens. Figure 8 gives the illustration of the same.

Decarburized layers at the surface of the heat-treated specimens are removed by machining and then used for

laser quenching process. Preheating at 100 °C and 160 °C is done for original/as-received sample and quenched and low temperature tempered specimen before laser hardening. Laser processing parameters, power 2 kW, scanning speed 1.2 m/min and beam size 3 mm × 8 mm , are kept constant for the entire study. Characterization analysis divulges the hardened depth for the four specimens in the order 0.46, 0.48, 0.67 and 0.66 mm, and this is due to different microstructures for different samples. Specimen quenched and low tempered and preheated at 160 °C before laser processing achieved case hardness above 0.7 mm [54]. Laser hardening of 100Cr6 steel with and without the presence of fluid is carried out in this study. Spheroidization annealing treatment is done before laser hardening. A rectangular beam of size 20 mm × 5 mm irradiated on the surface and the entire experiment is carried out in the presence of argon shielding gas. Laser beam power of 3.2 kW and 1.20 m/min scanning speed are identified parameters and kept constant for the entire experimentation. Case depth and hardened value achieved without fluid presence reported 0.5 mm and 950HV, which is comparatively higher than the hardening done under the fluid medium. Martensite refinement greatly influences the compressive residual stress and hardness of the treated surface [55].

Almost all laser beams are Gaussian, and however, in specific cases, it tends to be gainful to have a non-Gaussian irradiance profile. A decrease in symmetric irradiation is one of the drawbacks of the Gaussian profile beam. Gaussian beams always end up with excessive energy higher than the threshold required for the application and also energy lower than the threshold in the outer portions, and this is the key reason why' flat-top laser beam is advantageous at certain situations. By introducing optical means, the Gaussian laser beam is transformed into a flat-top laser beam and then focussed on the 35CrMo steel. Line beam of dimensions 17 mm × 1 mm achieved with the optical flats. At 2 kW power and 1.1 m/min hardened depth of 1.6 mm achieved, the hardness at the surface level was found to be 730 HV. Figure 9 shows the difference between a Gaussian laser beam and flat-top head laser beam [56].

Laser transformation hardening of EN43A steel is investigated using five different laser beam profiles. Neither the circular beam or the rectangular beam resulted an optimum profile. Various beam geometries considered for the study are shown in Fig. 10. More martensitic phase exhibited when a triangular type laser beam profile is used for hardening. The hardness value resulted using the a triangular profile is around 590 ± 10 HV comparatively higher than the other laser beam profiles [57].

Hardened depth and hardness at the laser processed surface are greatly influenced by laser power, scanning speed and focal distance. Response surface methodology is used to validate the same by carrying out the tests using central composite design (CCD) five-level RSM design with three parameters. Increased hardened area reported at high power, low scanning speed and minimum focal distance. Optimized parameters to conduct laser hardening at AISI 410 surface are 1.6 kW, 0.33 m/min and 63.35 mm focal plane distance. The hardness value of 670 HV and case depth 0f 2.4 mm are achieved at the optimized parameters [58].

A uniform layer of carbon is deposited using electrophoretic deposition method on the AISI 4130 steel cylindrical billet of 65 mm diameter and 10 mm thickness. A rectangular beam of dimensions 8 mm × 1.5 mm is focussed on the substrate surface from the laser head, positioned exactly at 60 mm from the sample surface. For the same input parameters, carbon-coated samples exhibited high martensitic phase than the uncoated samples. Maximum hardness value of 813

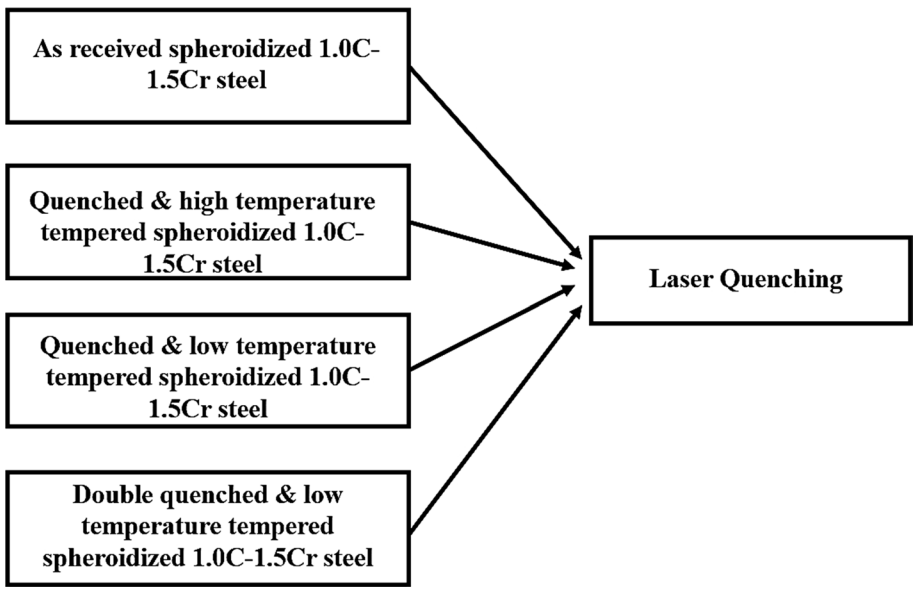

Fig. 8 Specimens preparation for laser quenching

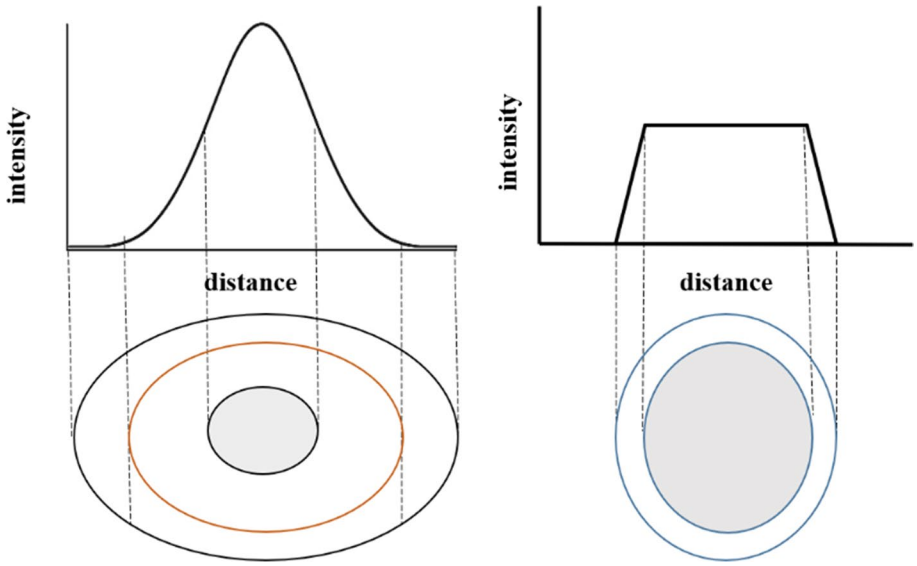

Fig. 9 Gaussian beam and flat top head beam

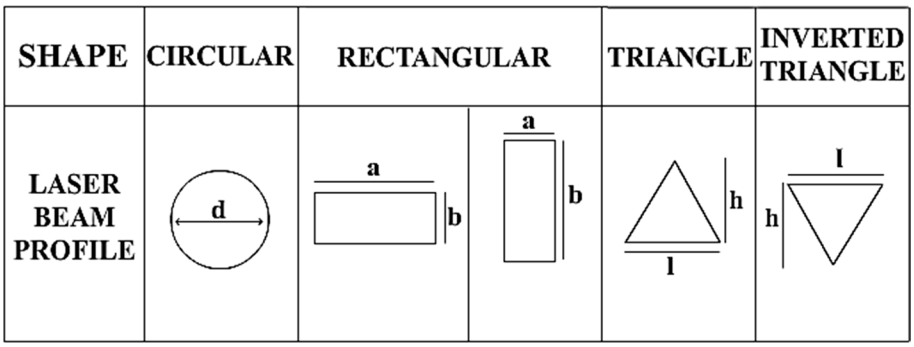

Fig. 10 Laser beam profiles used for transformation hardening of EN43A steel. *d—diameter of the circular beam; *a and b—corresponding rectangular' beam length and width; *l and h—corresponding triangular' beam base width and height

HV is reported on the carbon coated samples, comparatively higher than the uncoated samples 752 HV [59].

Laser transformation hardening of AISI 4130 steel using a rectangular beam of size 8 mm × 1.5 mm and a circular beam of spot size 0.25 mm is compared for their corresponding influence in hardened region geometry, microhardness and ferrite percent. Comparatively, higher case width and depth are achieved using a high-power diode laser type. Maximum hardness value of 792 HV with 1.02 mm depth is reported using a diode type hardening, and a maximum hardness value of 698 HV with 0.98 mm depth is reported using a Nd:YAG type hardening [60].

3.4.1 Precis

Rectangular type of laser beam is irradiated on the substrate surface in most of the high-power diode surface hardening treatments. With minimum power, desired depth and hardness are achieved on the base material. Laser hardening with an inert gas atmosphere is more effective in some cases. Surface hardness, wear resistance and corrosion resistance are significantly improved.

3.5 Surface treatment by fiber laser

Wide research work and investigations have been carried out and reported in the area of laser surface hardening with CO_2, Nd: YAG lasers and diode laser to date. Laser hardening with CO_2 and Nd: YAG lasers as a source is expensive, and the frequent need for surface coatings before laser irradiation to increase absorption is mandatory. High-power diode laser comparatively requires less cost, but the operating time is a concern. Operating costs of fiber laser are typically reduced to half of what a CO_2 system can offer, and this is due to the lower electrical consumption and high electrical efficiency of fiber lasers.

A high-power fiber laser YLS-3000 is used to surface harden the AISI 1045 steel. The shielding gas Argon is supplied onto the substrate surface. Hardening is done at a pressure of 0.5 MPa to avoid oxidization at high temperature. Surface cleaning is done with acetone to remove impurities and treated at ambient environment without preheating. Laser power, scanning speed of the laser head and focal plane distance are the parameters selected for this investigation, and the experiment trials are based on CCD proposed

by RSM and the same is power range 0.3–1.2 kW, speed range 0.18–0.72 m/min. Significant improvement in hardness is reported, i.e., around 660HV. Microstructure analysis reveals the typical structure formed during laser hardening, i.e., martensite transformation with finer grains and fractions of retained austenite varies with power, scanning and focal distance [61].

Investigation of surface hardness along with corrosion behavior of a laser-treated 50CrMo4 steel grade at a constant depth interval of 30 µm is done. Ytterbium-based fiber laser with 1.07 µm wavelength is focussed on the substrate surface at a distance of 290 (i.e., 10 mm defocus during laser irradiation). All the trials are carried out in an environment with Argon and the same being supplied at the rate of 15 l/min on the irradiated region through a nozzle. The laser power concentration and scanning speed are kept constant at 1.02×10^5 W/cm^2 and 3 m/min. The hardened layer containing iron and chromium oxides covers the entire scanned surface, nodes of rich Mn, Si and Cr formed at the undulation edges, and the presence of oxides reveals that argon shrouding doesn't influence the laser hardening process. Cross-sectional analysis reveals case depth of 0.5 mm achieved with 700 HV hardness value at < 0.1 mm depth, and the value decreases when the distance from the top end is increased. Experiments indicate that better corrosion resistance was achieved from the oxide layer [62].

Laser melting at a controlled atmosphere of argon gas was followed by 1 h tempering between the temperatures 500 °C and 900 °C done on the tool steel H13. Single-track melting method was adopted in this study with the following parameters, laser power 0.4–0.6 kW, scanning speed 0.2–1.6 m/min and a spot diameter of 3 mm for the entire experimentations. In laser melting, due to the rapid quenching, i.e., high-temperature gradient exists between the melted surface and the bulk, martensite and carbides microstructures are formed, and the same are finer than the conventionally hardened steel. It is also reported that the remelt layer experiences an austenitic transformation during the heating cycle, and when air-cooled, it gets hardened due to martensite formation. Tempering is done at a temperature larger than austenitization, i.e., > 850 °C ferrite/martensite peaks get weakened, and some oxide and carbide peaks may appear at the top surface, and this leads to a reduction in hard martensite phase at the top surface, and this could be the reason for reduced microhardness near the top surface. Hardness value more than 850 HV is achieved at 900 °C tempering [63].

Oxidation cannot be considered lightly in laser surface hardening. However, in most of the cases, laser hardening is done at atmospheric conditions and it also improves the mechanical properties of the material subjected. Laser hardening with controlled atmosphere gains interest since it influences the final microstructures on the surface resulted from hardening. Laser hardening is done in four different air, Argon, carbon dioxide and propane atmospheres to study their influence on the hardened layer. Hardening of AISI 1020 steel is carried out with same sets of parameters (power 0.25 kW, scanning speed 0.6 m/min and 0.5 mm beam diameter) for all the four cases. Case depth values reported are < 0.2 mm for all the four cases. The maximum hardness value of 914HV is achieved with propane environment laser hardening, and minimum hardness value of 350HV is achieved with carbon dioxide environment laser hardening. Argon-induced laser hardening resulted in 458HV hardness in the air, and it is 395HV at the surface. Significant improvement in hardness in propane(C_3H_8) environment may be due to carbon diffusion during hardening [64].

Laser transformation hardening of 1CD-5 tool steel is done by a YFL-600, a single-mode fiber laser. 0.5 kW power, scanning speed range 0.12–0.42 m/min. and 4.2 mm beam diameter are parameters chosen for this study. Experiments are carried out the substrate by (i) fixed power density and varying transverse speed, (ii) varying power density (by changing the focal plane position) and fixed transverse speed. Power density highly influences the hardened area. Case depth of 0.75 mm with 930HV is reported for fixed power density and varying transverse speed experiments and 0.9 mm depth with 920HV for varying power density and fixed transverse speed [65].

A camshaft is an integral part of an IC engine. The intended function of the camshaft is to open and close the inlet and valve at precision timing. The camshaft is prone to wear since it will be in continuous contact during the engine run. Nickel chromium alloy steel and Silchrome steel are the material for the inlet and exhaust valve. Due to continuous contact, the camshaft surface should be free from surface asperities, and the surface should be highly wear resistant. Laser surface hardening effect is investigated on GOST 801–78 steel, a camshaft material. Laser hardening technique and laser hardening technique followed by tempering are the two different approach of this study. Ytterbium fiber laser LS-15 (IPG) with the maximum output power of 15 kW is selected laser source. Power range 2.5–7.25 kW, 1.2 m/min transverse speed and 5.3° tilt angle (to avoid reflection) are the identified parameters. Hardened layers with 1 mm and 0.8 mm depths are reported for laser hardening without subsequent low-temperature tempering, and laser hardening with subsequent low-temperature tempering and the corresponding hardness values for the same are 825HV and 625 HV [66].

3.5.1 Precis

Laser power density, the scanning speed of the laser beam, focal plane distance are the parameters that have to be considered for laser surface treatment irrespective of the laser

type. Extensive work has to be carried out in fiber laser type surface hardening.

Figures 11, 12 and 13 show the case depths and microhardness of various laser surface hardened steel grades.

3.6 Influence of laser transformation hardening on wear and corrosion behavior of various steel grades

Hardness, abrasion resistance and corrosion resistance are the expected primary outcomes of engineering parts for industrial applications. By conventional treatment, the above requirements can be met but with the expense some mechanical attributes of the subjected material. Thermal distortion is another concern with conventional techniques. Laser surface hardening provides a tailor-made surface with good mechanical properties for various applications. Table 4 gives a consolidated description of the behavior of laser hardened samples toward the wear and corrosion environments.

3.7 Effect of laser parameters on the geometry of the hardened region

Various experiments have been successfully carried out to interpret the relation between the laser input parameters on the geometry of the hardened region. Some of the main equations of laser transformation hardening process are presented and discussed below.

Laser beam (circular type) interaction time with the substrate surface is given by Eq. (1) [51],

$$\text{Interaction time} = \text{Beam diameter(mm)}/\text{Scanning speed (mm/s)} \quad (1)$$

From the above relation, it is understood that laser beam interaction time is inversely proportional to the laser head scan speed. By varying the scanning speed, interaction time between the laser head and substrate surface can be altered. In other words, if the scan speed is high, interaction time is low, and if the scan speed is low, interaction time is high. Laser interaction time defines the final microstructure of the hardened surface.

Energy density of the laser can be obtained from the following relation Eq. (2) [68]; the below relation can be used for the rectangular or line laser beam geometry.

$$\text{Laser density}\left(\text{J/mm}^2\right) = \text{Laser Power (W)}/\{\text{Beam depth (mm)} \times \text{Scanning speed (mm/s)}\} \quad (2)$$

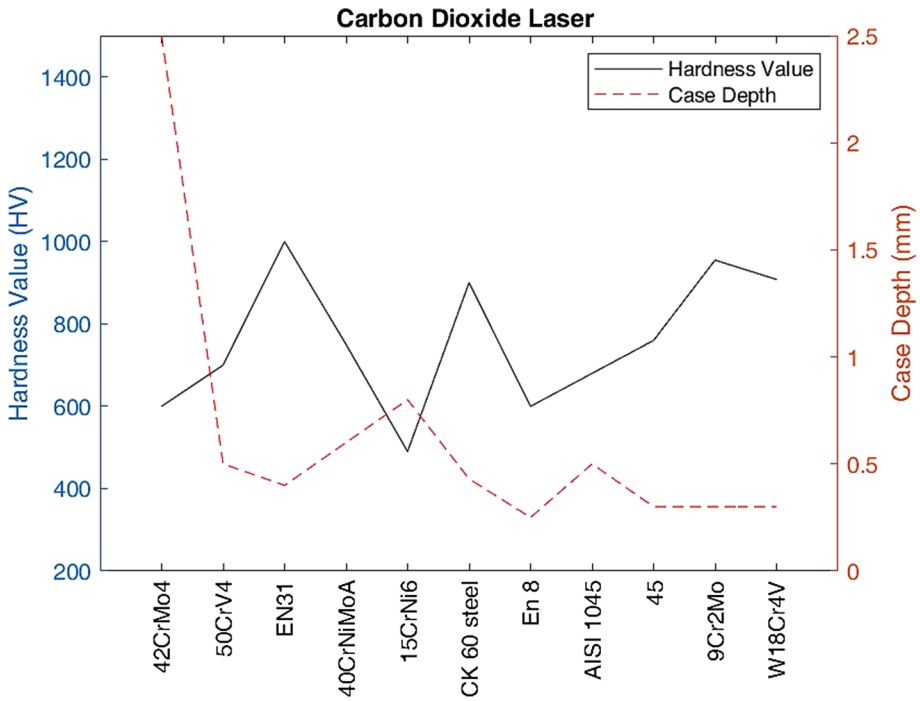

Fig. 11 Case depth and hardness values of various steel grades subjected to CO_2 laser surface hardening

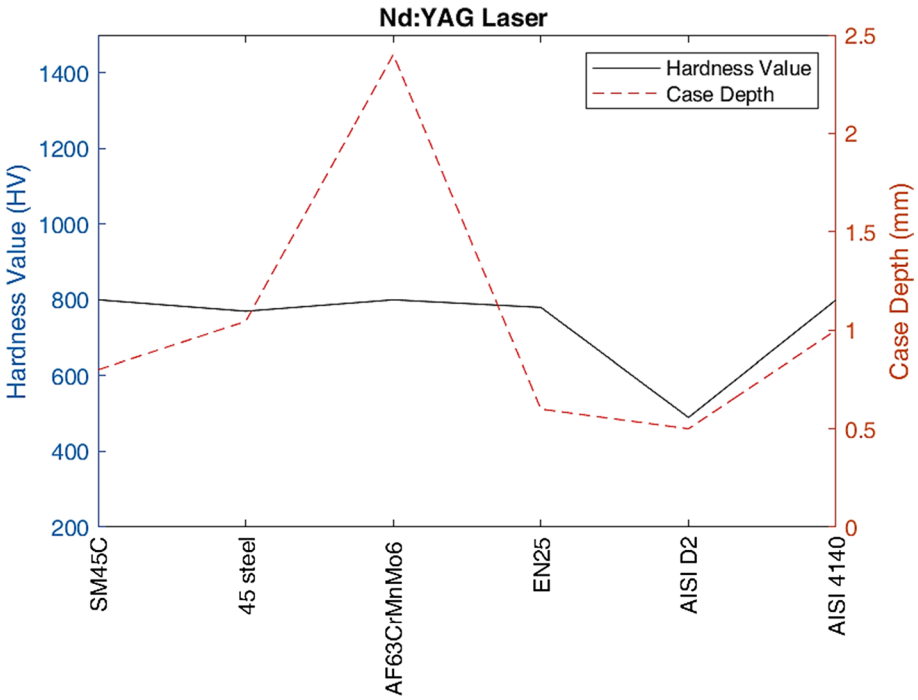

Fig. 12 Case depth and hardness values of various steel grades subjected to Nd: YAG laser surface hardening

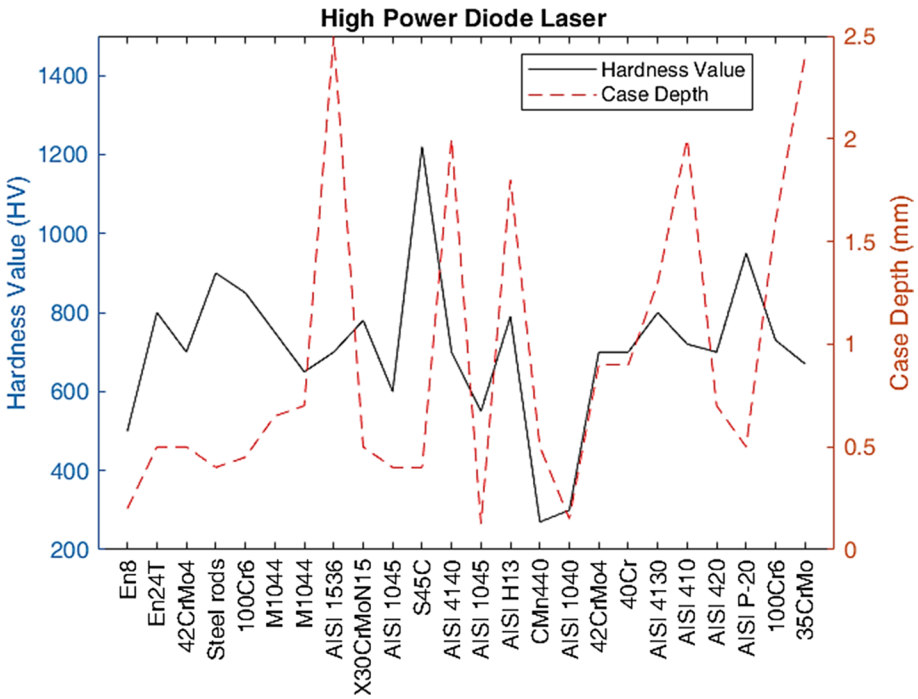

Fig. 13 Case depth and hardness values of various steel grades subjected to high-power diode laser surface hardening

The value of laser energy density can be also calculated using the obtained values of laser power and area together with interaction time for which the laser is directed on the substrate surface, and the same is shown in Eq. (3). The below equation can be used for a circular type laser beam geometry.

$$\begin{aligned}&\text{Laser density}\left(\text{J/mm}^2\right)\\&=\left\{\left(\text{Laser power (W)}\right)/\text{area}\left(\text{mm}^2\right)\right\}\\&\times\left\{\left(\text{Beam diameter(mm)}/\text{Scanning speed(mm/s)}\right\}\end{aligned}\tag{3}$$

Heat input and surface absorption are the two deciding factors of laser transformation hardening of various steel

Table 1 Surface hardening by CO_2 laser

Year	Steel grade	Carbon content reported (%)	Power range (used) (kW)	Beam type	Beam dimensions (mm)	Scanning speed range (m/min)	Pre-process treatment	Vickers hardness	Case depth achieved (mm)	Residual stress	Overlapping	Reference
1986	AISI 1045 AISI 4140	0.44 & 0.38	6–13	Circular & Line	Ø8 & 10×10, 16×16	0.5–5	Hardened and tempered	> 550HV	–	Tensile residual stresses at the laser hardened surface	–	[11]
1993	42CrMo4	0.42	–	–	-	–	Hardened and tempered & sand blasted	600HV	2.5 mm for both the cases	Tensile residual stresses at the laser hardened surface and overlapping regions are softened due to tempering	25% & 50%	[12]
1994	50CrV4	0.48	2.5	Square beam	15×15	0.7–1.4	Hardened and tempered & coated with black paint	700HV	0.5	Tensile residual stresses reported at the laser hardened surface	–	[13]
1997	EN31	1	1	Circular	Ø5	1.2	Hardened and tempered	1000HV	0.4	–	–	[15]
1998	40CrNiMoA	0.38	1.4	–	–	1.8	Hardened and black organic coated	750HV	0.6	–	–	[16]
1999	15CrNi6	0.15	1.5 & 3	Circular	Ø2–Ø7	3 to 18	Sandblasted & sandblasted + graphite coating	> 490HV	0.3–0.4 for sandblasted specimen & 0.6–0.8 for sandblasted + graphite-coated specimen	–	–	[17]

Table 1 (continued)

Year	Steel grade	Carbon content reported (%)	Power range (used) (kW)	Beam type	Beam dimensions (mm)	Scanning speed range (m/min)	Pre-process treatment	Vickers hardness	Case depth achieved (mm)	Residual stress	Overlapping	Reference
2002	CK 60 steel	0.6	1.5–3	Circular	Ø4–Ø6.5	1 to 6	3.5% wt. NaCl solution at room temperature applied on the surface before laser treatment	900HV	0.05–0.43	–	0% and 38% exhibit better wear resistance results	[18]
2004	AISI 1045	0.4	0.16	Circular	Ø 0.3	15.6–18	Sand blasted	768 HV	–	–	–	[19]
2005	En 8	0.38	2	Line	15×1	0.9	Normalized steel and thermo-absorptive coated	500–600 HV	0.14–0.25	–	–	[20]
2006	C45	0.45	0.35	Circular	Ø4	1.2	Zirconia coated	–	0.2	–	–	[21]
2007	C30, C40, C45	0.28,0.40,0.46	1.1–2.5	Circular	Ø1–Ø6	0.36—0.9	–	Considerable increase in hardness	0.05–1.55	–	–	[22]
2008	AISI 1045	0.4	1.1 & 1.2	Circular	Ø8	0.3–0.4	Graphite coated	680HV	0.5	–	50% overlap with 2 passes, 70% overlap with 3 passes and 75% overlap with 3 passes	[23]
2010	45, 9Cr2Mo and W18Cr4V	0.42–0.50, 0.85–0.95, 0.7–0.8	4	Circular	Ø5.5	4 m/min with 5minutes delay between the passes	Cleaned with acetone and coated with 10 wt% hydroxyethyl cellulose, 10 wt% titanium dioxide powder and 80 wt% talcum powder	760HV, 955HV, 908HV	<0.3	–	20% overlapping Tempering softening happens in overlapping zone	[24]

Table 2 Surface hardening by Nd: YAG laser

Year	Steel Grade	Carbon content reported (%)	Power range (used) (kW)	Beam type	Beam dimensions (mm)	Scanning speed range (m/min)	Pre-process treatment	Vickers hardness	Case depth achieved (mm)	Residual stress	Overlapping	Reference
2001	X30CrMoN15	0.3	–	Line	14 × 1.8	–	Hardened and tempered	–	–	Tensile at the surface & compressive below the hardened region	–	[25]
2009	SM45C	0.42–0.48	1–2	Circular	Ø2.8 & Ø5	0.054	–	800 HV	0.8	–	10–70%	[27]
2010	45 steel	0.42–0.50	0.4–0.6	Circular	Ø3	0.3	–	770 HV	1.044	–	–	[28]
2011	AF63CrMnMo6	0.62	2.5	Circular	Ø4	0.3	Hardened and tempered	800 HV	2.4	–	–	[29]
2012	14 (Ni) 200 grade maraging steel	< 0.008	1–3	Circular	Ø3–Ø6	1.5,3,3.6	Hardened and tempered & aging treatment	365 HV	–	–	25%	[30]
2013	EN25	0.31	0.75–1.5	Circular	Ø1.55	0.5, 0.75, 1	–	780 HV	0.6	–	–	[31, 32]
2014	AISI D2	1.64	1, 1.2 and 1.4	Circular	Ø2–Ø5	0.012–0.016	–	490 HV	0.5	–	–	[33]
2016	AISI 4140	0.38–0.43	1.8	Circular	Ø16	0.25	Hardened and tempered	800 HV	1	–	25% and 31%	[34]
2019	Cr12	2–2.3	0.6–2	Circular	–	0.36–0.72	–	–	1	–	–	[35]

Table 3 Surface hardening by HPDL

Year	Steel Grade	Carbon content reported (%)	Power range (used) (kW)	Beam type	Beam dimensions (mm)	Scanning speed range (m/min)	Pre-process treatment	Vickers hardness	Case depth achieved (mm)	Residual stress	Overlapping	Reference
2003	En8 & En24T	0.35–0.45	0.4–1	Rectangular	5×0.38	0.1–1.7	–	500 & 800 HV	0.2 & 0.5	–	–	[36]
2004	42CrMo4	0.42	0.65	–	–	–	–	700 HV	0.5	–	–	[37]
	42CrMoS4	0.38–0.45	0.2	Rectangular	0.8×5	0.025	–	–	–	–	–	
	4140 HT	0.38–0.43	2	–	–	–	–	–	1.9	–	–	
	Steel rods		–	–	–	–	–	900 HV	0.2–0.4	–	–	
	Automotive torsion springs	0.5–0.6	–	–	–	–	–	–	0.2–0.4	–	–	
	100Cr6	0.9–1.5	0.3	–	–	–	–	850 HV	0.45	–	–	
	M1044	0.43–0.50	1.4	Rectangular	11×2.8 and 22×2.8	0.5 & 0.2	–	750 HV,650 HV	0.65 & 0.7	–	–	
2006	AISI 1536	0.3–0.37	1.2	Rectangular	12×8	0.18	–	650–730 HV	1.5–2.5	–	–	[38]
2006	42CrMo4	0.44	1–2.72	Rectangular	5.3×12.3	0.3–0.6	Diamond polished and ethanol cleaned	–	0.5	–	–	[39]
	AISI 420L	0.21										
2007	X30Cr-MoN15	0.275	2 to 3	Rectangular	8×4	0.125	Hardened	780 HV	0.15–0.5	–	10–50%	[40]
2007	AISI 1045	0.42–0.5	0.47–0.76	Rectangular	1.7×3.8	0.3–1.5	–	600 HV	0.4	–	–	[41]
2009	S45C	0.45	0.443	Rectangular	0.23×1.82	0.02–0.04	Powder coating and infrared heat treatment	1220 HV	0.4	–	–	[42]
2008	AISI 4140	0.38–0.43	0.85	Rectangular	12×8	0.03	–	700 HV	2	–	50–75%	[43]
2014	AISI 1045	0.43	0.125	Rectangular	1.7×0.9	0.4	–	550 HV	0.125	Compressive residual stress	20%	[44]
2014 & 2015	AISI H13	0.32–0.45	0.9–2.5	Rectangular	20×5	0.12–0.48	Hardened and tempered	790 HV & 670 HV	1 & 1.8	Compressive residual stress	–	[45, 46]
2017	CMn440	0.1	0.7	Rectangular	4×4	0.72–1.92	Cold rolled & annealed	270	0.3–0.5	–	12.50%	[47]
2017	AISI 1040	0.37–0.44	0.2	Ellipse	1.9×0.6	0.72–1.2	–	300 HV	0.15	–	–	[48]
2018	42CrMo4	0.44		Rectangular	25.8×7.8		Normalized	700 HV	0.9	–	–	[49]
2018	40Cr	0.44	1.15	Rectangular	25×6	0.48	–	700 HV	0.9	–	–	[50]
2019	AISI 4130	0.25	1.2–1.5	Rectangular	*varying	0.18–0.42	–	800 HV	1.3	–	30% 7 50%	[51]

Table 3 (continued)

Year	Steel Grade	Carbon content reported (%)	Power range (used) (kW)	Beam type	Beam dimensions (mm)	Scanning speed range (m/min)	Pre-process treatment	Vickers hardness	Case depth achieved (mm)	Residual stress	Overlapping	Reference
2019	AISI 410 & AISI 420	0.15 & 0.2	1.2–1.6	Rectangular	*varying	0.3 & 0.36	–	650 HV & 720 HV	2 & 1.3	–	–	[52]
2019	AISI P-20	0.38	1.25	Rectangular	25 × 1	0.3		700 HV	0.7	–	–	[53]
2020	1.0C–1.5Cr	1	2	Rectangular	3 × 8	1.2	Hardened & tempered	–	0.7	–	–	[54]
2020	100Cr6	0.9–1.5	3.2	Rectangular	20 × 5	1.2	–	950 HV	0.5	–	–	[55]
2020	35CrMo	0.32–0.40	2	Line	17 × 1	1.1	–	730 HV	1.6	–	–	[56]
2020	AISI 410	0.15	1.6	Rectangular	–	0.33	–	670 HV	2.4	–	–	[57]
2019	AISI 4130	0.25	1.6	Rectangular	8 × 1.5	0.18–0.3		813 HV	1.5	–	–	[59]
2020	AISI 4130	0.25	1.6	Rectangular *Circular (Nd: YAG laser)	8 × 1.5 *0.25 mm	0.18–0.3	–	792 HV 698 HV	1.02 0.98	–	–	[60]

grades. The generalized equation for heat input for laser transformation hardening is given by Eq. (4) [60],

$$\text{Heat Input} = \text{Power(W)}/\text{Scan speed (mm/s)} \quad (4)$$

During surface hardening, continuous heat is directed on to the substrate surface and this makes the surface to reach the austenitic region and austenite particle are formed during the same. Then, by sudden cooling (self-quenching) martensite phase is obtained.

The following relations Eqs. (5) and (6) can be used for pulsed mode laser hardening technique [70, 71].

$$\text{Pulse energy(J)} = \text{Laser Power (average)(W)}/\text{Laser pulse frequency (Hz)} \quad (5)$$

$$\text{Peak power(kW)} = \text{Pulse energy (J)/Pulse width (ms)} \quad (6)$$

3.8 Numerical simulation on laser transformation hardening

Developing a heat source model for laser hardening is a challenging task. Various researchers have done the numerical simulation model and predicted the outcome of the process. Along with that, experimental validation is also done. Table 5 shows the sequential development of numerical models on laser transformation hardening technique.

3.9 Laser transformation hardening technique in industrial applications

A clean manufacturing environment with superior quality is the main reason for the industries to opt for a state of the heart "laser-assisted manufacturing." Materials processing such as heat treatment, hard facing, alloying and cladding are dominant in the modern-day industry. Advantages of laser hardening over conventional hardening are already discussed in section "Introduction" with Figs. 3 and 4. Table 6 depicts the industrial applications of laser surface hardening.

4 Laser surface processing—upcoming scopes and challenges

Laser transformation hardening is a widely used surface modification technique of ferrous metals for the past two decades. When compared with conventional hardening treatments and mechanisms, laser surface modification is a straight forward technique. In conventional hardening, percentage of carbon is the deciding factor for most of the cases, whereas in laser hardening with a minimum percentage of carbon in the base/substrate selected (for example

Table 4 Wear and corrosion report of various laser hardened steel grades

Material	Laser type & beam geometry	Wear	Corrosion	Reference
EN31	CO_2 & Ø5 mm	Average weight loss per mm^2(grams); unhardened—0.027; hardened—0.013. significant improvement in wear resistance	–	[15]
40CrNiMoA	CO_2 & Ø6 mm	Wear resistance of laser quenched samples is 1.3 times higher than the normal samples High hardness and compressive type residual stress are the main reasons for the improvement in wear resistance	–	[16]
CK60	CO_2 & Ø4–Ø6.5 mm	Multi–track laser hardened specimens with 0% and 38% overlapping ratios showed improved wear resistance	Better corrosion behavior in NaCl environment exhibited by low overlapping ratio tracks	[18]
EN8 steel	CO_2 & 15 × 1 mm	During the dry sliding wear tests, laser surface hardened EN8 steel specimens exhibited greater wear resistance than conventionally hardened specimens (around 10^{-13} to 10^{-12} m^3/min)	–	[20]
X30CrMoN15	Nd: YAG & 14 × 1.8 mm	Wear resistance improvement is attributed predominantly due to the stability of the oxide layer formation supported by the substrate	–	[25]
AISI 420	Nd: YAG (pulsed)	–	Dissolving of carbide from grain boundaries into grains leads to the formation of discontinuous grain boundaries reported after the laser hardening and this causes the corrosion potential to dissolve and results in higher corrosion resistance	[67]
14 Ni (200 grade)	Nd: YAG & Ø3–Ø6mm	Laser surface melting (LSM) + aging heat treatment resulted an enhancement in the hardness and in the wear resistance; the surface layer of the laser melted track resulted with 0.28mm^3 volume loss, which is comparatively less than the base metal 0.52 mm^3	–	[30]
EN25	Nd: YAG & Ø1.55 mm	Formation of martensite phase results in high hardness at the contact surface. For all the experimental conditions, laser hardened samples exhibited less wear, in contrast with the as-received samples	–	[32]
X30CrMoN15	HPDL & 8 × 4 mm	–	Laser hardening with argon as shrouding atmosphere improves the corrosion resistance of the steel, but a slight decrease in hardness near the surface is also reported	[40]
AISI H13	HPDL & 20 × 5 mm	Laser hardening resulted in a superior fretting wear behavior and also a reduced coefficient of friction as compared to that in as-received AISI H13	Marginal reduction in corrosion rate compared to that in the as received samples. E_{corr} values of laser engineered samples are − 910 to − 920 mV SCE as compared to that of as received AISI H13 steel − 960 mV SCE	[46]
AISI P-20	HPDL & 24 × 1 mm	Maximum wear resistance was noticed for the surface hardened with low power density	Marginal increase in corrosion resistance is also reported for the laser hardening with low power density. Comparative increase in corrosion resistance is noted for both the low power and high power densities when compared with that of the base metal	[68]
SAE52100	HPDL (CW& PW) & 20 × 5 mm	PW mode laser hardening exhibited a substantial improvement in hardness and sliding wear resistance	–	[69]

Table 4 (continued)

Material	Laser type & beam geometry	Wear	Corrosion	Reference
100Cr6	HPDL (CW & PW) & 20×5 mm	Great reduction in wear reported in laser treated surfaces, owing to high resistance to shear and plastic deformation induced by high strength martensitic microstructure	–	[55]

*CO_2, carbon dioxide; Nd: YAG, Neodymium-doped Yttrium Aluminum Garnet; HPDL, high-power diode laser

15CrNi6, AISI410, AISI420) desired surface microstructures (diffusion-less transformations) and properties are achieved. Another important criterion important is surface topography and surface absorptivity. If the surface roughness value is < 35 µm, hardening has no effect on the surface. Surface coating is mandatory for CO_2 lasers since its wavelength is higher than Nd: YAG, diode and fiber lasers. One of the reasons this technique is an immense accomplishment in industrial sectors is because it does not deal with bulk material treating. Selected areas are irradiated with the laser source for repairs and surface modifications, and uniform case depth is achieved for the entire processed area/section, which is still a difficult task in conventional hardening. Case hardened layers are highly wear and corrosion resistant.

Highlights of laser surface modifications are:

(1) Speed and accuracy—a desired requirement at the industry level
(2) Uniform case depth over the treated surface
(3) Tailor-made surface properties of the substrate for a chosen application
(4) No quenching medium/self-quenching
(5) Minimum distortion
(6) Diffusion-less transformations
(7) No post-treatment requirement
(8) Power density, scanning speed decide the hardened area.

Although laser treatment has several benefits, it also has few hindrances, and they are:

(1) Cost factor
(2) Mandatory surface coating
(3) Radiation shielding
(4) Additional care must be given for high reflective materials
(5) Skilled labor-extensive knowledge is required to operate.

5 Back tempering

Back tempering is another phenomenon that is to be considered. When the surface area for laser treatment becomes high, it is tough to find the optimal distance between the two single tracks on the surface every time. Multitrack with overlap is the solution for this scenario. But most of the studies have reported that overlapping/back tempering results in the reduction in surface hardness at some particular sections. A parametric optimization is an approach that can overcome overlapping hindrances. The typical heat source model for laser type hardening is a Gaussian type, and it is not

Table 5 Chronological development of numerical models on laser transformation hardening

Material	Focus of the work	Model type	Software used	Heat source model adopted	Reference
AISI 1045	Effects of Gaussian beam mode and a square beam mode on induced residual stresses at the substrate surface during laser hardening are done using FEM	2D	New 2D finite element model (*1989)	Gaussian and square	[72]
C45	Temperature filed in LTH numerically simulated. Various laser beam energy densities are analyzed for optimum parameter. FEM model is adopted	3D	MSC. Marc	Heat flux density distribution—circular spot	[21]
C45	FEM is used to compute the solution for the heat distribution and phase transformation and also to find the optimum overlapping parameters	3D	SYSWELD	Gaussian distribution—moving heat source model	[73]
Inconel 718 alloy	Temperature and stress fields in the laser focussed regions are predicted using FEM and validated with experimentation	3D	ABAQUS	Gaussian distribution—moving heat source model	[74]
GCr15	FEM–residual stress filed and temperature field in laser hardening are simulated and analyzed by adopting the theory of elastic plasticity, Mises yielding criterion and isoclinic hardening criterion and validation experiment results are in good agreement with the simulated results	3D	ANSYS	Linear spot heat flow distribution	[75]
AISI 4340	(i) Examination of the temperature distribution using heat diffusion equations, boundary conditions and material properties (ii) Discretization of the mathematical model by adopting finite difference method (iii) Validation by using experimental tests and simulation with COMSOL Multiphysics software	3D	COMSOL	Gaussian beam distribution	[76]
AISI 4130	A finite element model was employed for the simulation of the LSTH Results showed that the model can predict the temperature profile and the size and the shape of the laser hardened region with good accuracy	3D	Simu fact welding 8.0 (MSC Software)	Gaussian beam distribution	[71]

necessary to have only a Gaussian. For LTH, a flat top-hat model is another choice. Gaussian model is more successful for heat treatments such as welding, but, in the case of laser hardening and laser melting, flat top-hat model may be the better choice, since it covers the large surface area and minimal energy loss. Process parameter selection is a vital step in that process. Multi-track hardening for the large surface area is shown in Fig. 14. Several overlap ratios 0%, 30%, 40%, 50% and 70% are investigated, but 0% overlap ratio is reported with good result when compared with other overlap ratio percentage. Care must be taken so that the hardening does not end up with melting and cracks. Higher case depth

Table 6 Industrial applications of laser surface hardening

Material	Laser type and specification	Laser beam geometry	Outcome	Reference
AISI 410	CW CO_2; 15 kW	Circular; Ø1 mm	Surface hardening of martensitic stainless steel turbine blade is successfully carried out Good metallurgical result with the absence of cracks is reported	[77]
40CrNiMoA	CW CO_2, 2 kW	–	Laser hardened piston heads in diesel power plants showed a significant improvement in wear resistance, and it is an effective way to prolong the service	[16]
2Cr13	CW CO_2; 3 kW	Circular; Ø4 mm	Improvement in impact wear resistance of laser surface-processed steel was attributed due to grain refinement and also due to the presence of higher martensite content	[78]
AISI H13	CW Fiber; 200 W	Circular; Ø0.08 mm	Significant improvement in the surface hardness (X 2times). Tool industry applications	[79]
45 Hot-rolled steel	HLD1001.5 solid-state laser; Nd: YAG 1 kW CW	Circular; Ø3 mm	Disk openers showed excellent wear resistance after the laser hardening	[28]
GCr15	CW CO_2	Rectangular—3.5 × 2.5 mm	Laser hardening successfully performed on the GCr15 steel ring. The ring can be used in industrial components like bearings, precision measuring tools, dies, rotating devices, machines and automobiles. Three times increase in hardness is reported	[80]
SAE 52,100 steel	CW CO_2; 9 kW	Rectangular—17.5 × 0.6 mm	Compressive type residual stress and high hardness and wear resistance without affecting the bainitic core are reported	[81]
AISI 420B	CW fiber laser; 5 kW	Circular; Ø9 mm	Laser heat treatment of an industrial axisymmetric hollow mechanical part successfully done	[82]
AISI 5135	CW $CO_{2,\ 3}$ kW	Circular; Ø3 mm	Threefold increase in hardness of the gear steel when compared with the base metal and subsequently increase wear resistance	[83]

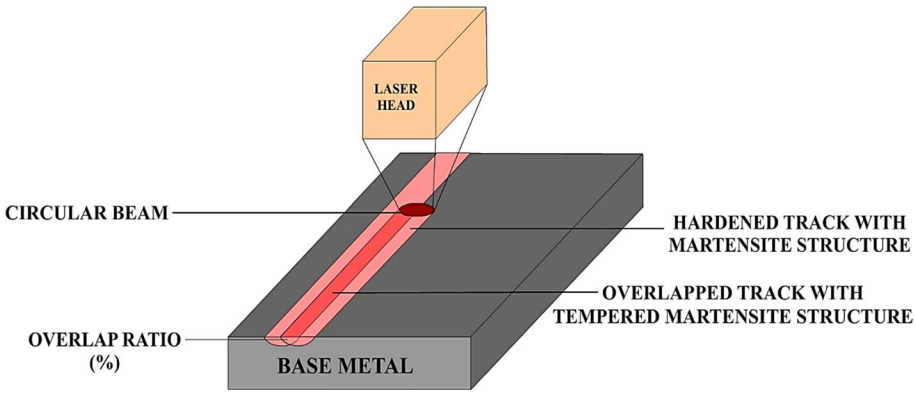

Fig. 14 Multi-track hardening technique for large surface area

with no cracks is a challenging task. Almost all the laser hardening ends up with tensile residual stress at the surface and compressive stress under the hardened layer, and this is due to the diffusion-less transformation of the austenite phase to martensite accompanied with a change in volume of the substrate steel.

6 Conclusions

- Steels are a perfect candidate for laser surface hardening.
- Laser transformation hardening is the widely adopted technique to modify the surface of the selected steels using a laser source.

- Hardened zone, transition zone, heat-affected zone are an integral part of the hardened layer resulted from laser transformation hardening.
- Various research concluded that the case-hardened depth is in the range 0.15–2.3 mm for laser surface hardening.
- Microhardness resulted from laser hardening technique is superior than the base metal subjected.
- Hardness at various zones can be given by
- **hardened zone > transition zone > heat-affected zone > base metal**
- Back tempering is still a concern in laser hardening that involves in multi-tracks.
- Wear resistance is significantly improved after laser hardening for many cases.
- Various researchers reported significant compressive stress are all over the hardened layer, a martensitic region bounded by tensile stresses. The compressive stress resulted in the hardened region is mainly because of volumetric dilatation of the material transforming into martensite. The residual stress formation is the result of plastic deformation and flow due to thermal expansion and contraction (due to large temperature gradient) and volume changes due to phase transformations.
- Laser hardening at a controlled atmosphere is the new method of approach for increasing the mechanical properties at the substrate surface. Laser hardening done at controlled atmosphere reported valid and gained better results.
- From the review, it is evident that laser power, scanning speed, focal plane distance are the parameters that influence the hardened layer one way or the other. High-power fiber lasers proved that they are a likely candidate for producing high surface hardness and hardened depth for various steels. Extensive study is required in fiber laser optimization with an appropriate optics and scanning parameters.

References

1. Ion JC (1996) Process diagrams for laser transformation hardening. In: Mazumder J, Conde O, Villar R, Steen W (eds) Laser processing: surface treatment and film deposition. Springer Netherlands, Dordrecht, pp. 587–612. https://doi.org/10.1007/978-94-009-0197-1
2. Babu PD, Balasubramanian KR, Buvanashekaran G (2011) Laser surface hardening: a review. Int J Surf Sci Eng 5:131–151. https://doi.org/10.1504/ijsurfse.2011.041398
3. Woo HG, Cho HS (1999) Three-dimensional temperature distribution in laser surface hardening processes. Proc Inst Mech Eng B J Eng Manuf 213:695–712. https://doi.org/10.1243/0954405991517128
4. Grum J, Šturm R (1997) Laser surface melt-hardening of gray and nodular irons. Appl Surf Sci 109–110:128–132. https://doi.org/10.1016/S0169-4332(96)00648-4
5. Caron-Guillemette G (2010) A review of the use of lasers in transformation hardening. https://doi.org/10.13140/RG.2.1.3114.6642
6. Pantsar H (2006) Henry Granjon Prize Competition 2006 Co-Winner, Category A "Joining and fabrication technology" models for diode laser transformation hardening of steels. Weld World 50:3–11. https://doi.org/10.1007/BF03263440
7. Canning J (2006) Fibre lasers and related technologies. Opt Lasers Eng 44:647–676. https://doi.org/10.1016/j.optlaseng.2005.02.008
8. Limpert J, Röser F, Schreiber T, Manek-Hönninger I, Salin F, Tünnermann A (2006) Ultrafast high power fiber laser systems. Comptes Rendus Phys 7:187–197. https://doi.org/10.1016/j.crhy.2006.01.016
9. Dinesh Babu P, Buvanashekaran G, Balasubramanian KR (2012) Experimental studies on the microstructure and hardness of laser transformation hardening of low alloy steel. Trans Can Soc Mech Eng 36:241–257. https://doi.org/10.1139/tcsme-2012-0018
10. Safdar S, Li L, Sheikh MA, Liu Z (2005) An analysis of the effect of laser beam geometry on laser transformation hardening. J Manuf Sci Eng 128:659–667. https://doi.org/10.1115/1.2193547
11. Solina A, de Sanctis M, Paganini L, Coppa P (1986) Residual stresses induced by localized laser hardening treatments on steels and cast iron. J Heat Treat 4:272–280. https://doi.org/10.1007/BF02833305
12. de Freitas M, Pereira MS, Michaud H, Pantelis D (1993) Analysis of residual stresses induced by laser processing. Mater Sci Eng A 167:115–122. https://doi.org/10.1016/0921-5093(93)90344-E
13. Belló JM, Fernández BJ, López V, Ruiz J (1994) Fatigue performance and residual stresses in laser treated 50CrV4 steel. J Mater Sci 29:5213–5218. https://doi.org/10.1007/BF01151119
14. Yoon K-K, Kim W-B, Na S-J (1996) Shape deformation of a piston ring groove by laser surface hardening. Surf Coatings Technol 78:157–167. https://doi.org/10.1016/0257-8972(94)02403-0
15. Zhang XM, Man HC, Li HD (1997) Wear and friction properties of laser surface hardened En31 steel. https://doi.org/10.1016/s0924-0136(97)00011-3
16. Liu Q, Song Y, Yang Y, Xu G, Zhao Z (1998) On the laser quenching of the groove of the Piston head in large diesel engines. J Mater Eng Perform 7:402–406. https://doi.org/10.1361/105994998770347855
17. Katsamas aI, Haidemenopoulos GN (1999) Surface hardening of low-alloy 15CrNi6 steel by CO_2 laser beam. Surf Coatings Technol 115:249–255. https://doi.org/10.1016/S0257-8972(99)00246-7
18. Pantelis DI, Bouyiouri E, Kouloumbi N, Vassiliou P, Koutsomichalis A (2002) Wear and corrosion resistance of laser surface hardened structural steel. Surf Coatings Technol 161:125–134. https://doi.org/10.1016/S0257-8972(02)00495-4
19. Cheung N, Pinto MA, Ierardi MCF, Garcia A (2004) Mathematical modeling and experimental analysis of the hardened zone in laser treatment of a 1045 AISI steel. Mater Res 7:349–354. https://doi.org/10.1590/s1516-14392004000200022
20. Kaul R, Ganesh P, Tiwari P, Nandedkar RV, Nath AK (2005) Characterization of dry sliding wear resistance of laser surface hardened en 8 steel. J Mater Process Technol 167:83–90. https://doi.org/10.1016/j.jmatprotec.2004.09.085
21. Wang XF, Lu XD, Chen GN, Hu SG, Su YP (2006) Research on the temperature field in laser hardening. Opt Laser Technol 38:8–13. https://doi.org/10.1016/j.optlastec.2004.11.005
22. Rana J, Goswami GL, Jha SK, Mishra PK, Prasad BVSSS (2007) Experimental studies on the microstructure and hardness of

laser-treated steel specimens. Opt Laser Technol 39:385–393. https://doi.org/10.1016/j.optlastec.2005.07.001
23. Tani G, Orazi L, Fortunato A (2008) Prediction of hypo eutectoid steel softening due to tempering phenomena in laser surface hardening. CIRP Ann Manuf Technol 57:209–212. https://doi.org/10.1016/j.cirp.2008.03.057
24. Yao C, Xu B, Huang J, Zhang P, Wu Y (2010) Study on the softening in overlapping zone by laser-overlapping scanning surface hardening for carbon and alloyed steel. Opt Lasers Eng 48:20–26. https://doi.org/10.1016/j.optlaseng.2009.05.001
25. Heitkemper M, Fischer A, Bohne C, Pyzalla A (2001) Wear mechanisms of laser-hardened martensitic high-nitrogen-steels under sliding wear. Wear 250–251:477–484. https://doi.org/10.1016/S0043-1648(01)00659-7
26. Vuorinen E, Pino D, Lundmark J, Prakash B (2007) Wear characteristic of surface hardened Ausferritic Si-steel. J Iron Steel Res Int 14:245–248. https://doi.org/10.1016/S1006-706X(08)60087-4
27. Kim JDo, Lee MH, Lee SJ, Kang WJ (2009) Laser transformation hardening on rod-shaped carbon steel by Gaussian beam. Trans Nonferrous Met Soc China (English Ed) 19:941–945. https://doi.org/10.1016/S1003-6326(08)60382-9
28. Sun H, Ling G, Li HW, Su, YB, Xiong SP, Yao HR (2010) The influence of laser hardening on the microstructure and wear resistance of disk opener. In: Manufacturing Science and Engineering I, pp 1497–1501. Trans Tech Publications Ltd (2010). https://doi.org/10.4028/www.scientific.net/amr.97-101.1497
29. Pellizzari M, Flora MGD (2011) Influence of laser hardening on the tribological properties of forged steel for hot rolls. Wear 271:2402–2411. https://doi.org/10.1016/j.wear.2011.01.044
30. Cabeza M, Castro G, Merino P, Pena G, Román M (2012) Laser surface melting: a suitable technique to repair damaged surfaces made in 14 Ni (200 grade) maraging steel. Surf Coatings Technol 212:159–168. https://doi.org/10.1016/j.surfcoat.2012.09.039
31. Dinesh Babu P, Buvanashekaran G, Balasubramanian KR (2012) Experimental investigation of laser transformation hardening of low alloy steel using response surface methodology. Int J Adv Manuf Technol 67:1883–1897. https://doi.org/10.1007/s00170-012-4616-z
32. Babu PD, Buvanashekaran G, Balasubramanian K (2013) Dry sliding wear of laser hardened low alloy steel at room and elevated temperatures. Proc Inst Mech Eng J J Eng Tribol 227:1138–1149. https://doi.org/10.1177/1350650113481530
33. Jai Hindus S, Hema Kumar S, Xavier Arockiyaraj S, Venkatesh Kannan M, Kuppan P (2014) Experimental investigation on laser assisted surface tempering of AISI D2 tool steel. Procedia Eng 97:1489–1495. https://doi.org/10.1016/j.proeng.2014.12.432
34. Cordovilla F, García-Beltrán Á, Sancho P, Domínguez J, Ruiz-de-Lara L, Ocaña JL (2016) Numerical/experimental analysis of the laser surface hardening with overlapped tracks to design the configuration of the process for Cr-Mo steels. Mater Des 102:225–237. https://doi.org/10.1016/j.matdes.2016.04.038
35. Wang Q, Zeng X, Chen C, Lian G, Huang X (2019) Profile characterisation and response surface modelling of laser surface hardened Cr12 mould steel. Procedia Manuf 34:168–176. https://doi.org/10.1016/j.promfg.2019.06.135
36. Pashby IR, Barnes S, Bryden BG (2003) Surface hardening of steel using a high power diode laser. J Mater Process Technol 139:585–588. https://doi.org/10.1016/S0924-0136(03)00509-0
37. Kennedy E, Byrne G, Collins DN (2004) A review of the use of high power diode lasers in surface hardening. J Mater Process Technol 155–156:1855–1860. https://doi.org/10.1016/j.jmatprotec.2004.04.276
38. Skvarenina S, Shin YC (2006) Predictive modeling and experimental results for laser hardening of AISI 1536 steel with complex geometric features by a high power diode laser. Surf Coatings Technol 201:2256–2269.. https://doi.org/10.1016/j.surfcoat.2006.03.039
39. Pantsar H, Kujanpää V (2006) Effect of oxide layer growth on diode laser beam transformation hardening of steels. Surf Coatings Technol 200:2627–2633. https://doi.org/10.1016/j.surfcoat.2004.09.001
40. Van Ingelgem Y, Vandendael I, Van den Broek D, Hubin A, Vereecken J (2007) Influence of laser surface hardening on the corrosion resistance of martensitic stainless steel. Electrochim Acta 52:7796–7801. https://doi.org/10.1016/j.electacta.2007.02.011
41. Lusquiños F, Conde JC, Bonss S, Riveiro A, Quintero F, Comesaña R, Pou J (2007) Theoretical and experimental analysis of high power diode laser (HPDL) hardening of AISI 1045 steel. Appl Surf Sci 254:948–954. https://doi.org/10.1016/j.apsusc.2007.07.200
42. Morimoto J, Ozaki T, Kubohori T, Morimoto S, Abe N, Tsukamoto M (2008) Some properties of boronized layers on steels with direct diode laser. Vacuum 83:185–189. https://doi.org/10.1016/j.vacuum.2008.03.102
43. Lakhkar RS, Shin YC, Krane MJM (2008) Predictive modeling of multi-track laser hardening of AISI 4140 steel. Mater Sci Eng A 480:209–217. https://doi.org/10.1016/j.msea.2007.07.054
44. Avilés R, Albizuri J, Ukar E, Lamikiz A, Avilés A (2014) Influence of laser polishing in an inert atmosphere on the high cycle fatigue strength of AISI 1045 steel. Int J Fatigue 68:67–79. https://doi.org/10.1016/j.ijfatigue.2014.06.004
45. Telasang G, Dutta Majumdar J, Padmanabham G, Manna I (2014) Structure-property correlation in laser surface treated AISI H13 tool steel for improved mechanical properties. Mater Sci Eng A 599:255–267. https://doi.org/10.1016/j.msea.2014.01.083
46. Telasang G, Dutta Majumdar J, Padmanabham G, Manna I (2015) Wear and corrosion behavior of laser surface engineered AISI H13 hot working tool steel. Surf Coatings Technol 261:69–78. https://doi.org/10.1016/j.surfcoat.2014.11.058
47. Syed B, Shariff SM, Padmanabham G, Lenka S, Bhattacharya B, Kundu S (2017) Influence of laser surface hardened layer on mechanical properties of re-engineered low carbon steel sheet. Mater Sci Eng A 685:168–177. https://doi.org/10.1016/j.msea.2016.12.124
48. Guarino S, Barletta M, Afilal A (2017) High Power Diode Laser (HPDL) surface hardening of low carbon steel: fatigue life improvement analysis. J Manuf Process 28:266–271. https://doi.org/10.1016/j.jmapro.2017.06.015
49. Soriano C, Alberdi G, Lambarri J, Aranzabe A, Yáñez A (2018) Laser surface tempering of hardened chromium-molybdenum alloyed steel. Procedia CIRP 74:353–356. https://doi.org/10.1016/j.procir.2018.08.140
50. Chen Z, Zhu Q, Wang J, Yun X, He B, Luo, J (2018) Behaviors of 40Cr steel treated by laser quenching on impact abrasive wear. Opt Laser Technol 103:118–125. https://doi.org/10.1016/j.optlastec.2018.01.039
51. Moradi M, KaramiMoghadam M (2019) High power diode laser surface hardening of AISI 4130; statistical modelling and optimization. Opt Laser Technol 111:554–570. https://doi.org/10.1016/j.optlastec.2018.10.043
52. Moradi M, Arabi H, Jamshidi S, Benyounis KY (2019) A comparative study of laser surface hardening of AISI 410 and 420 martensitic stainless steels by using diode laser. Opt Laser Technol 111:347–357. https://doi.org/10.1016/j.optlastec.2018.10.013
53. Park C, Kim J, Sim A, Sohn H, Jang H, Chun EJ (2019) Influence of diode laser heat treatment and wear conditions on the fretting wear behavior of a mold steel. Wear 434–435:202961. https://doi.org/10.1016/j.wear.2019.202961
54. Li ZX, Tong BQ, Zhang QL, Yao JH, Kovalenko V, Li ZG (2020) Influence of initial microstructure on the microstructure evolution and mechanical properties of 1.0C-1.5Cr steel in the laser

surface quenching. Mater Sci Eng A 788:139490. https://doi.org/10.1016/j.msea.2020.139490
55. Anusha E, Kumar A, Shariff SM (2020) A novel method of laser surface hardening treatment inducing different thermal processing condition for Thin-sectioned 100Cr6 steel. Opt Laser Technol 125. https://doi.org/10.1016/j.optlastec.2020.106061
56. Zhu H, Fu X, Fan S, Liang L, Lin X, Ning Y (2020) The conversion from a Gaussian-like beam to a flat-top beam in the laser hardening processing using a fiber coupled diode laser source. Opt Laser Technol 125:106028. https://doi.org/10.1016/j.optlastec.2019.106028
57. Safdar S, Li L, Sheikh MA, Liu Z (2006) An analysis of the effect of laser beam geometry on laser transformation hardening. J Manuf Sci Eng Trans ASME 128:659–667. https://doi.org/10.1115/1.2193547
58. Moradi M, Arabi H, Shamsborhan M (2020) Optik multi-objective optimization of high power diode laser surface hardening process of AISI 410 by means of RSM and desirability approach. Opt Int J Light Electron Opt 202:63619. https://doi.org/10.1016/j.ijleo.2019.163619
59. Moradi M, Karami Moghadam M, Kazazi M (2019) Improved laser surface hardening of AISI 4130 low alloy steel with electrophoretically deposited carbon coating. Optik (Stuttg) 178:614–622. https://doi.org/10.1016/j.ijleo.2018.10.036
60. Moradi M, Karami Moghadam M, Shamsborhan M (2020) How the laser beam energy distribution effect on laser surface transformation hardening process; Diode and Nd:YAG lasers. Optik (Stuttg). 204:163991. https://doi.org/10.1016/j.ijleo.2019.163991
61. Chen C, Zeng X, Wang Q, Lian G, Huang X, Wang Y (2020) Statistical modelling and optimization of microhardness transition through depth of laser surface hardened AISI 1045 carbon steel. Opt Laser Technol 124:105976. https://doi.org/10.1016/j.optlastec.2019.105976
62. Maharjan N, Murugan VK, Zhou W, Seita M (2019) Corrosion behavior of laser hardened 50CrMo4 (AISI 4150) steel: a depth-wise analysis. Appl Surf Sci 494:941–951. https://doi.org/10.1016/j.apsusc.2019.07.172
63. Patra Karmakar D, Gopinath M, Nath AK (2019) Effect of tempering on laser remelted AISI H13 tool steel. Surf Coatings Technol 361:136–149. https://doi.org/10.1016/j.surfcoat.2019.01.022
64. Maharjan N, Zhou W, Wu N (2020) Direct laser hardening of AISI 1020 steel under controlled gas atmosphere. Surf Coatings Technol 385:125399. https://doi.org/10.1016/j.surfcoat.2020.125399
65. Ameri MH, Ghaini FM, Torkamany MJ (2018) Investigation into the efficiency of a fiber laser in surface hardening of ICD-5 tool steel. Opt Laser Technol 107:150–157. https://doi.org/10.1016/j.optlastec.2018.05.030
66. Lasota I, Protsenko V, Matyushkin A, Kuznetsov M, Gook S (2020) Laser surface hardening of engine camshaft cams. Mater Today Proc, pp 1–5. https://doi.org/10.1016/j.matpr.2019.12.400
67. Mahmoudi B, Torkamany MJ, Aghdam ARSR, Sabbaghzade J (2010) Laser surface hardening of AISI 420 stainless steel treated by pulsed Nd:YAG laser. Mater Des 31:2553–2560. https://doi.org/10.1016/j.matdes.2009.11.034
68. Park C, Sim A, Ahn S, Kang H, Chun EJ (2019) Influence of laser surface engineering of AISI P20-improved mold steel on wear and corrosion behaviors. Surf Coatings Technol 377:124852. https://doi.org/10.1016/j.surfcoat.2019.08.006
69. Anusha E, Kumar A, Shariff SM (2020) Diode laser surface treatment of bearing steel for improved sliding wear performance. Optik (Stuttg). 206. https://doi.org/10.1016/j.ijleo.2019.163357
70. Khorram A, Davoodi A, Jafari A, Moradi M (2019) Nd: YAG laser surface hardening of AISI 431 stainless steel; mechanical and metallurgical investigation. Opt Laser Technol 119:105617. https://doi.org/10.1016/j.optlastec.2019.105617
71. Casalino G, Moradi M, Moghadam MK, Khorram A, Perulli P (2019) Experimental and numerical study of AISI 4130 steel surface hardening by pulsed Nd:YAG laser. Materials (Basel) 12. https://doi.org/10.3390/ma12193136
72. Technology C (1989) A study on residual stresses in laser surface hardening of a medium carbon steel. 38:311–324. https://doi.org/10.1016/0257-8972(89)90093-5
73. Rowshan R, Baán MK (2007) Thermal and metallurgical modelling of laser transformation hardened steel parts. In: Materials science, testing and informatics III, pp 599–606. Trans Tech Publications Ltd. https://doi.org/10.4028/www.scientific.net/msf.537-538.599
74. Yilbas BS, Akhtar SS, Karatas C (2010) Laser surface treatment of Inconel 718 alloy: thermal stress analysis. Opt Lasers Eng 48:740–749. https://doi.org/10.1016/j.optlaseng.2010.03.012
75. Lei S, Yan Y, Li H, Niu L, Gui ZX, Wu YB (2012) Numerical simulation of residual stress field in laser transformation hardening for GCr15 steel components and experimental study. In: Materials processing technology II. pp 1897–1903. Trans Tech Publications Ltd. https://doi.org/10.4028/www.scientific.net/amr.538-541.1897
76. Fakir R, Barka N, Brousseau J (2018) Case studies in thermal engineering case study of laser hardening process applied to 4340 steel cylindrical specimens using simulation and experimental validation. Case Stud Therm Eng 11:15–25. https://doi.org/10.1016/j.csite.2017.12.002
77. Camoletto A, Molino G, Talentino S (1991) Laser hardening of turbine blades. Mater Manuf Process 6:53–65. https://doi.org/10.1080/10426919108934735
78. Tianmin S, Meng H, Yuen TH (2003) Impact wear behavior of laser hardened hypoeutectoid 2Cr13 martensite stainless steel. Wear 255:444–455. https://doi.org/10.1016/S0043-1648(03)00417-4
79. Lee JH, Jang JH, Joo BD, Son YM, Moon YH (2009) Laser surface hardening of AISI H13 tool steel. Trans Nonferrous Met Soc China (English Ed) 19:917–920. https://doi.org/10.1016/S1003-6326(08)60377-5
80. Akhter R, Hussain A, Farooq WA, Aslam M (2010) Laser surface hardening of GCr15 bearing steel ring. Key Eng Mater 442:130–136. https://doi.org/10.4028/www.scientific.net/KEM.442.130
81. Basu A, Chakraborty J, Shariff SM, Padmanabham G, Joshi SV, Sundararajan G, Dutta Majumdar J, Manna I (2007) Laser surface hardening of austempered (bainitic) ball bearing steel. Scr Mater 56:887–890. https://doi.org/10.1016/j.scriptamat.2007.01.029
82. Tani G, Fortunato A, Ascari A, Campana G (2010) Laser surface hardening of martensitic stainless steel hollow parts. CIRP Ann - Manuf Technol 59:207–210. https://doi.org/10.1016/j.cirp.2010.03.077
83. Selvan JS, Subramanian K, Nath AK (1999) Effect of laser surface hardening on En18 (AISI 5135) steel. J Mater Process Technol 91:29–36. https://doi.org/10.1016/S0924-0136(98)00430-0